Microfluidic separations

Prof. Wim De Malsche
wim.de.malsche@vub.be

Department of Chemical Engineering

Outline

- Intro
- Flow propagation
  - Electro-osmotic flow
  - Shear-driven
  - Pressure
- Particle separation

INTRODUCTION

Why go small ? : Shortened Diffusion Times

$$d_{diff} = \sqrt{2 D_m t}$$

Molecular diffusion

distance	1 mm	1 µm	0.1 µm
time	1000 s	1 ms	0.01 ms

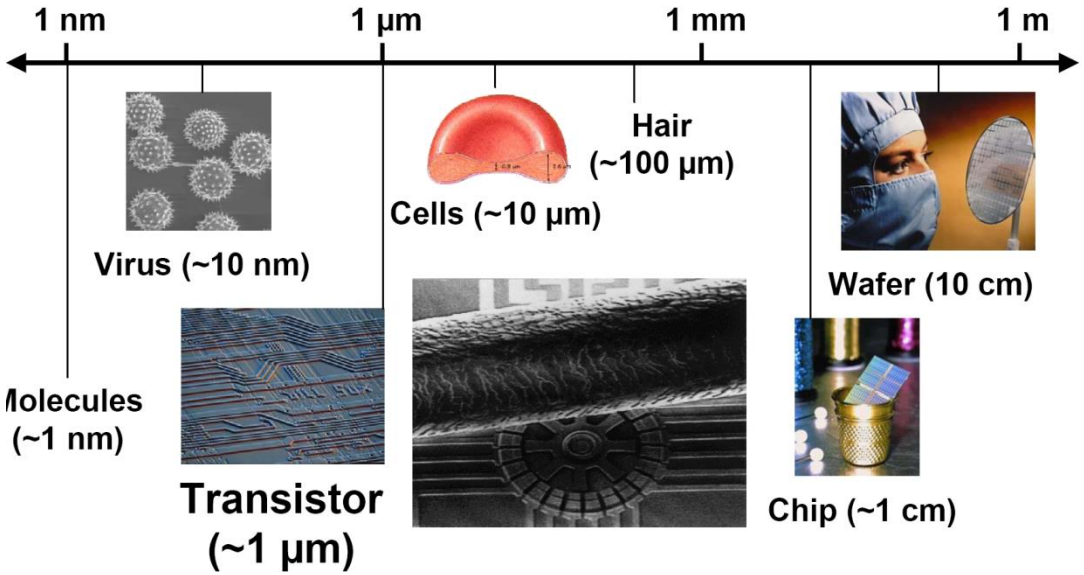

Chromatography terminology

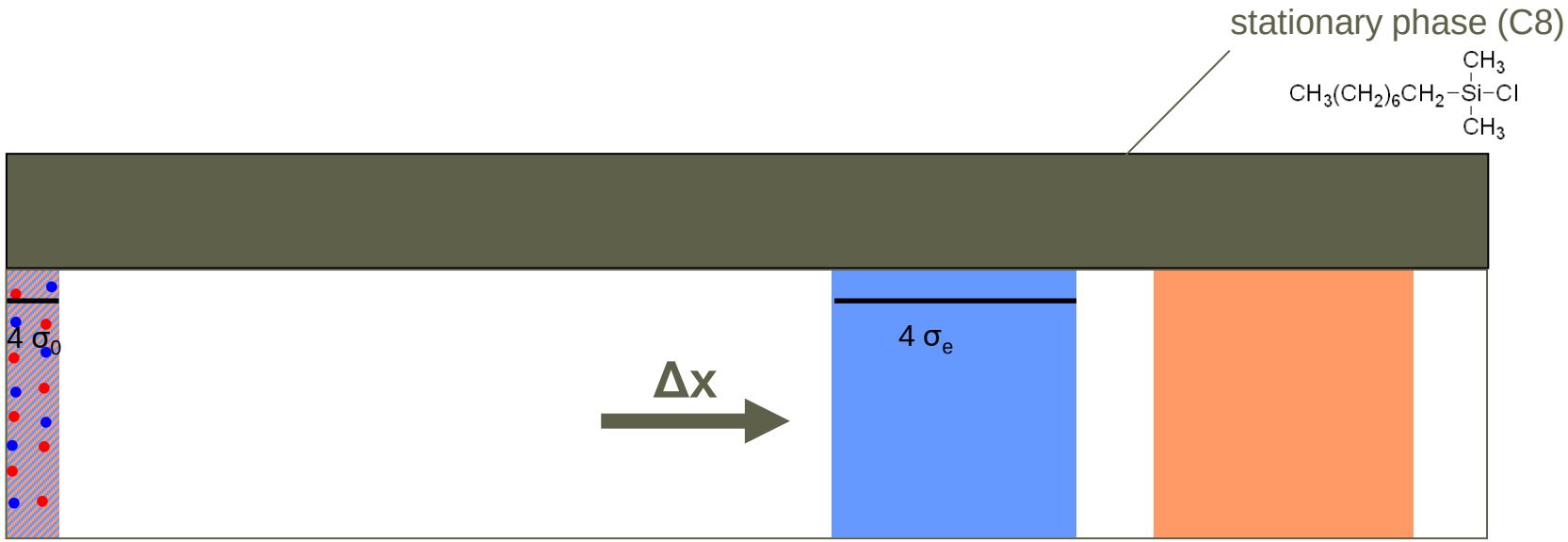

Plate height $H=\Delta\sigma^2/\Delta x$

Permeability: $K_v=u.\eta.L/\Delta P$

Retention coefficient $k'=(t_r-t_0)/t_0$

Peak capacity $PC\sim1/4.\ln(k'+1)\sqrt{N}$

van Deemter Equation

$$H = A + B/u + Cu$$

C-term is related to the mass-transfer resistance between the stationary-phase and the mobile phase

B-term is linked to the axial dispersion due to the molecular diffusion

A-term represents the heterogeneity of the system

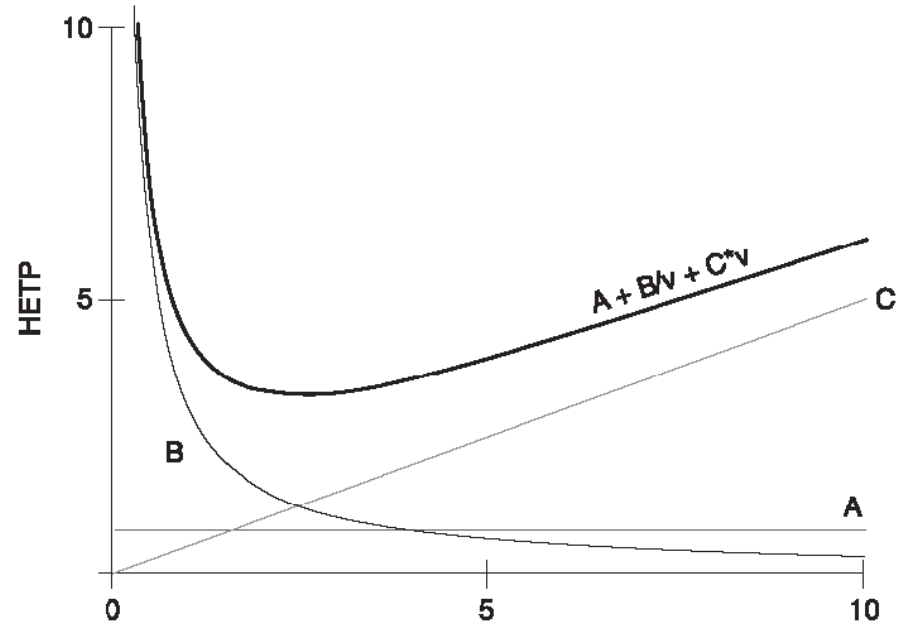

To compare between different column configurations, the reduced plate height ***h*** is defined

$$h = A + B/v + Cv \qquad h = \frac{H}{d_p} \qquad v = \frac{u d_p}{D_m}$$

d_p _particle diameter
D_m _diffusion coefficient
u _mobile phase velocity

FLOW PROPAGATION

Flow propagation

- Electro-osmotic flow
- Shear-driven
- Pressure

Flow propagation

- Electro-osmotic flow
- Shear-driven
- Pressure

Electroosmotic flow (EOF)

electrically-driven flow: → u usually independent of d

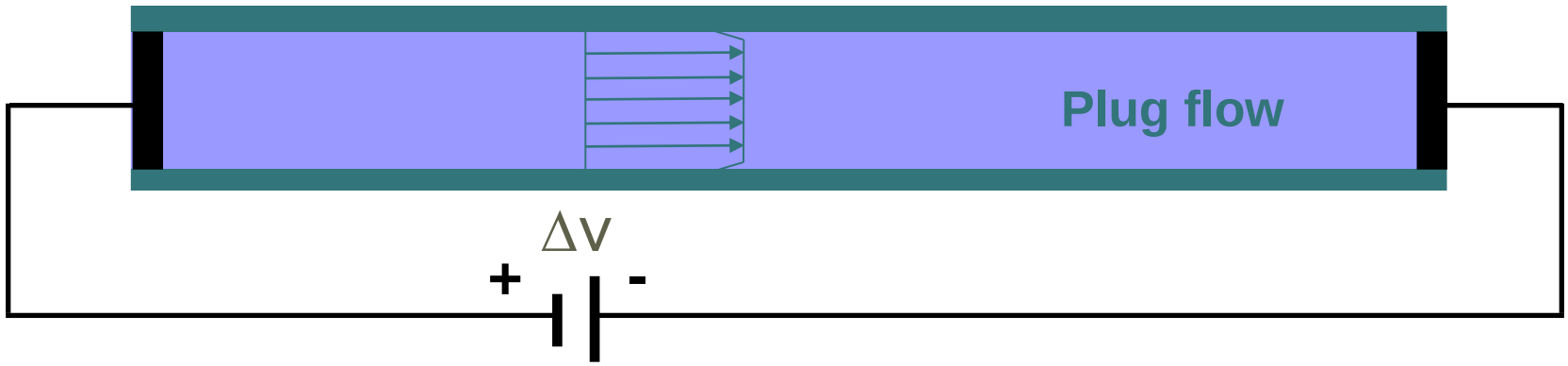

$$u_{eo} = -\frac{\varepsilon_o \varepsilon_e \zeta}{\eta} \cdot \frac{\Delta V}{L}$$

ζ: electric potential on surface

ΔV applied field strength (Max = 30 KV)

EOF principle

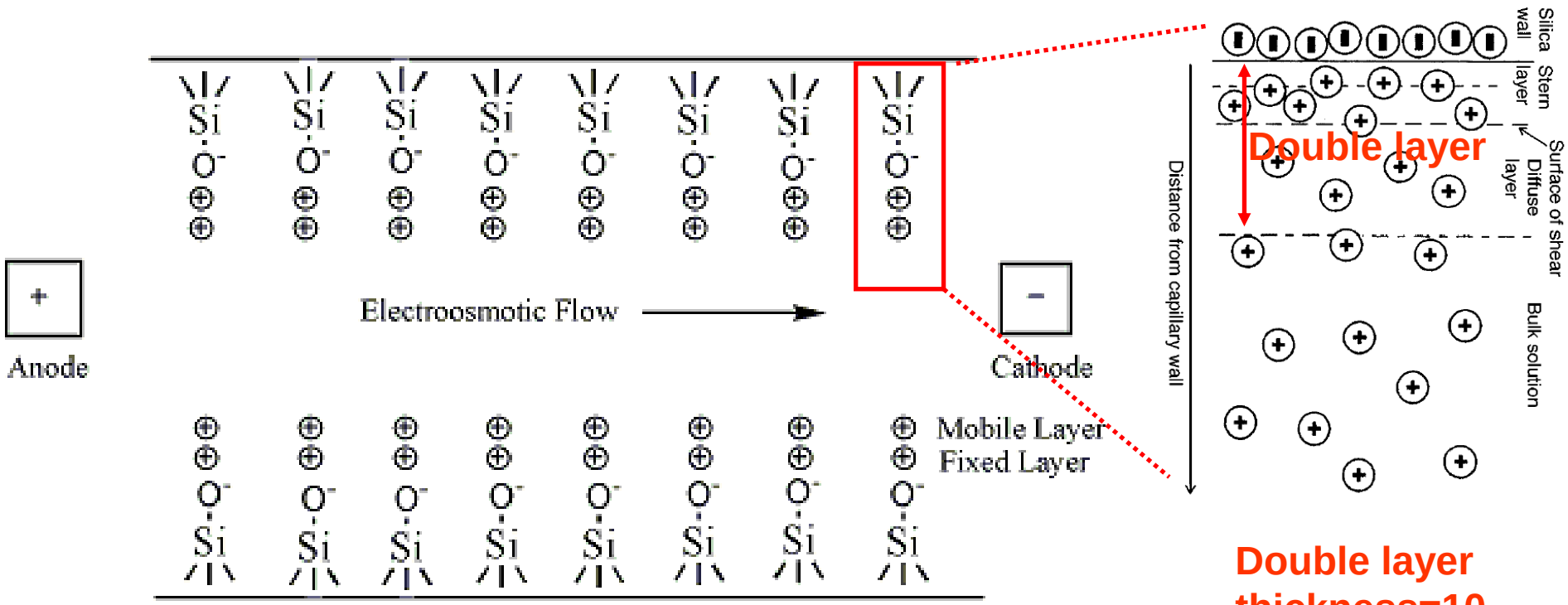

Double layer thickness=10-100 nm

$$u_{eo} = \frac{\varepsilon_0 \varepsilon_r \zeta}{\eta} \frac{\Delta V}{L}$$

$u_0 = \mu_0 E = = \mu_0 \Delta V/L$: velocity

μ_0 = electroosmotic mobility

ε_0, ε_r= dielectric constants vacuum, solvent

η: viscosity

ΔV: potential difference

L: length

COMOSS

Anal. Chem. **1998,** *70,* 3790−3797

Fabrication of Nanocolumns for Liquid Chromatography

Bing He,[†] Niall Tait,[‡] and Fred Regnier*,[§]

Department of Chemistry, Purdue University, Lafayette, Indiana 47907, Alberta Microelectronics Corporation, Edmonton, Canada T6G 2T9, and PerSeptive Biosystems, Framingham, Massachusetts 01701

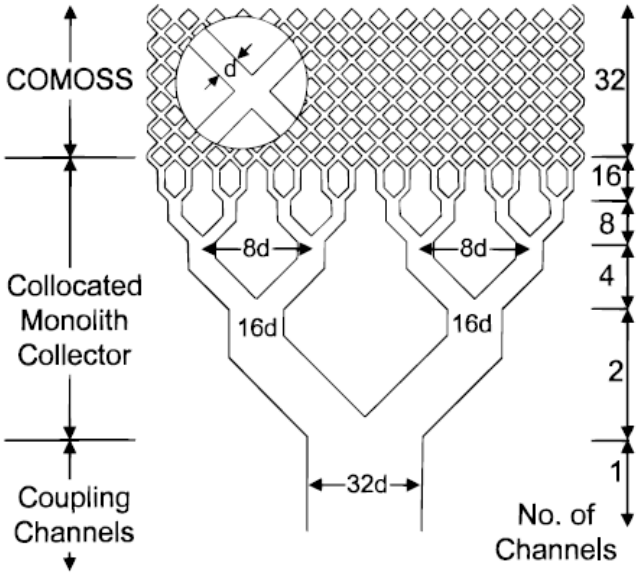

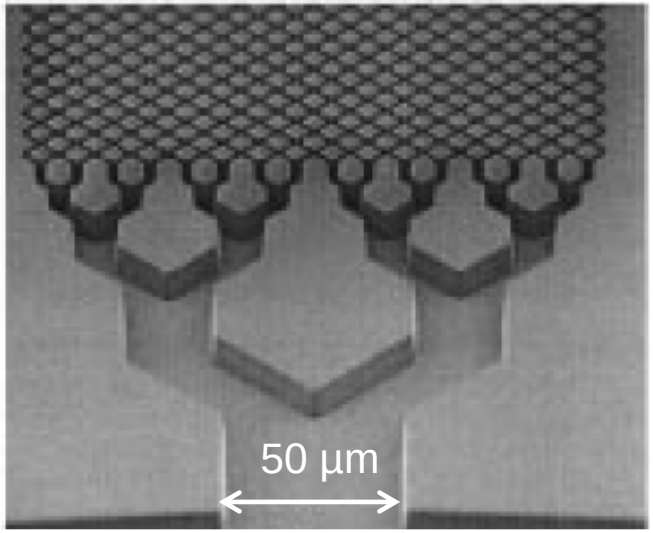

Pillar arrays for CEC: shape

J. Sep. Sci. 2002, *25*, 1011–1018 JOURNAL OF SEPARATION SCIENCE 1011

Benjamin E. Slentz,
Natalia A. Penner,
Fred Regnier

Geometric effects of collocated monolithic support structures on separation performance in microfabricated systems

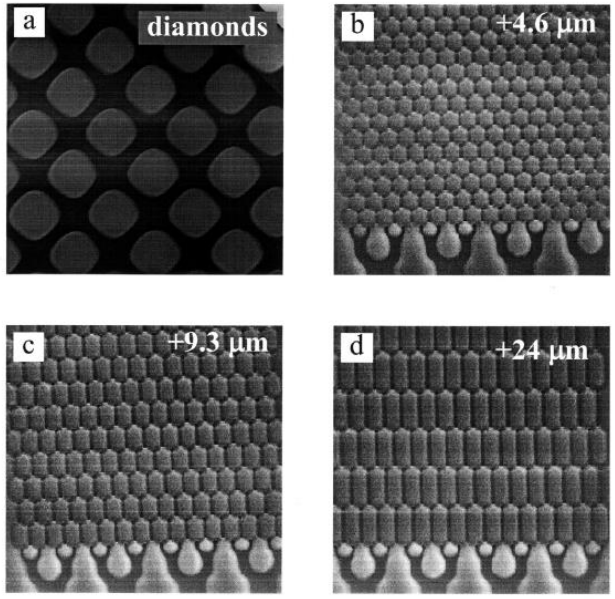

Figure 3. SEMs of a section of a diamond COMOSS column (a) and its extended hexagonal modifications with the extension lengths of 4.6 µm (b), 9.3 µm (c), and 24 µm (d).

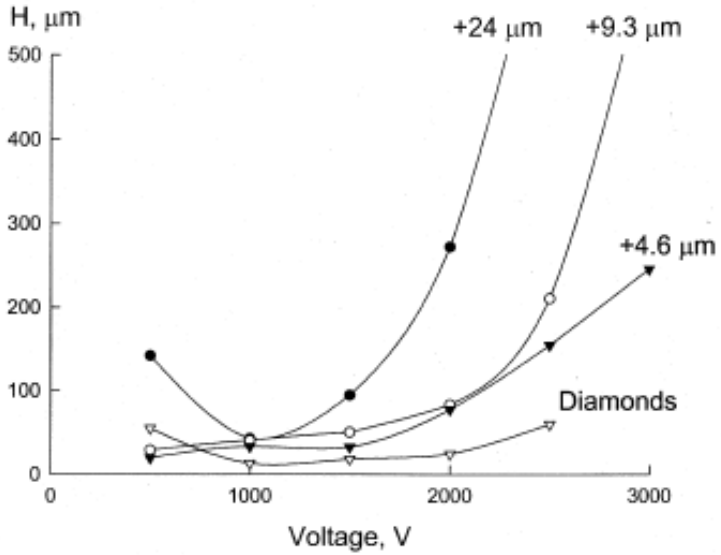

Figure 5. Plot of plate height (*H*) *vs.* voltage for the columns in Figure 3 modified with 4-styrenesulfonic acid. Model compound is rhodamine 110.

Pillar arrays for CEC: mobility

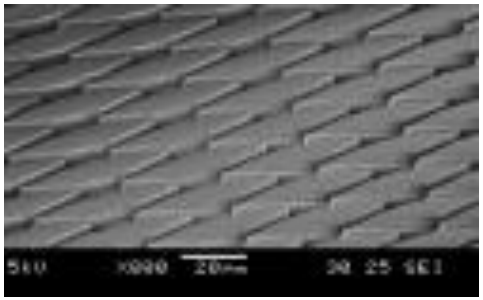

Pillar length	58.6 μm	45.4 μm	57.8 μm	39.3 μm
Pillar width	7.5 μm	7.5 μm	8.1 μm	7.5 μm
Wetted perimeter	236.7 μm	185.0 μm	233.3 μm	39.3 μm
Minimum spacing	2.37 μm	1.95 μm	2.17 μm	2.27 μm

$$d_{eq} = \sqrt{\frac{4A_p}{\pi}}$$

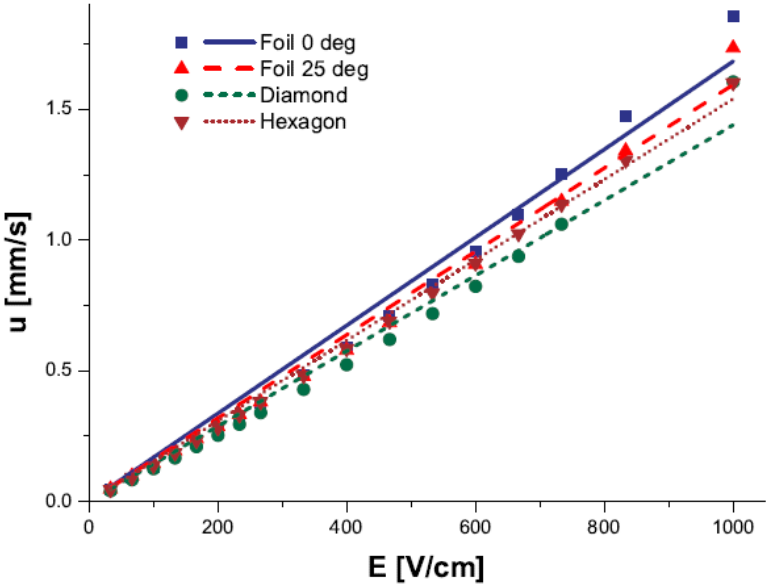

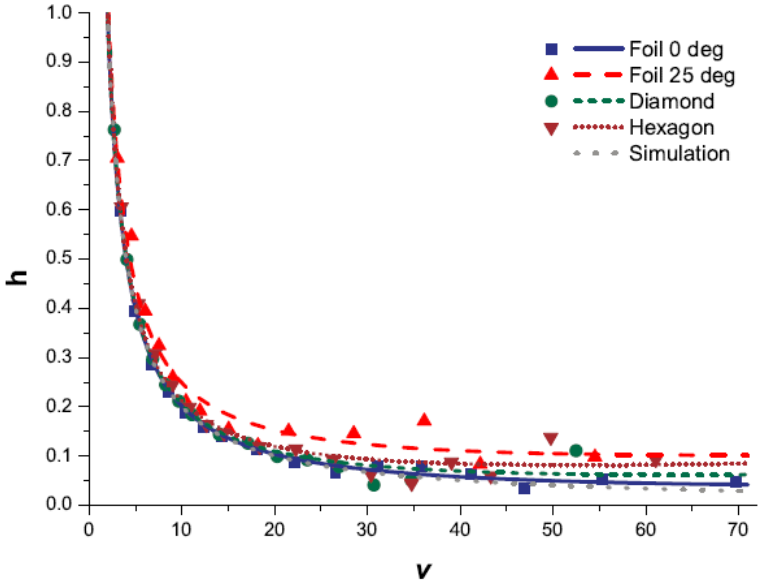

Sukas, S., De Malsche, W., Desmet,G., Gardeniers, J.G.E. (2012), Anal. Chem., 84, 9996-10004

Relevance high peak capacity

Only 14,000 human proteins identified (100,000 predicted)

Marginal progress during recent years*

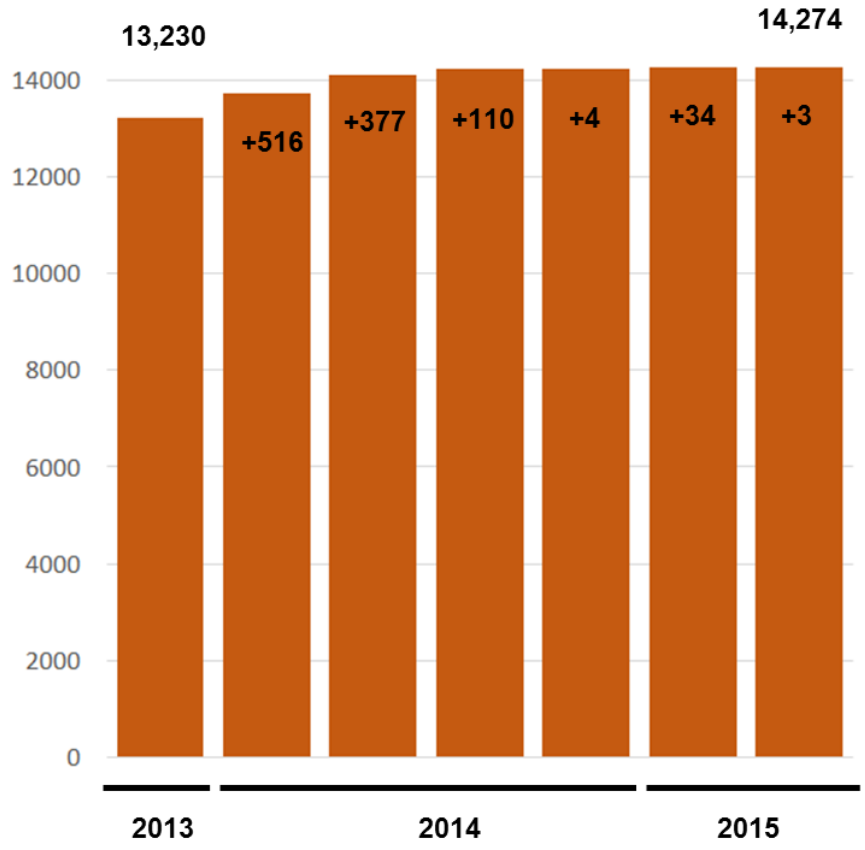

*Prof. Ruedi Aebersold,
HPLC conference, Geneve, 2015

CEC using pillars: $N_{max,\ k'=0}$?

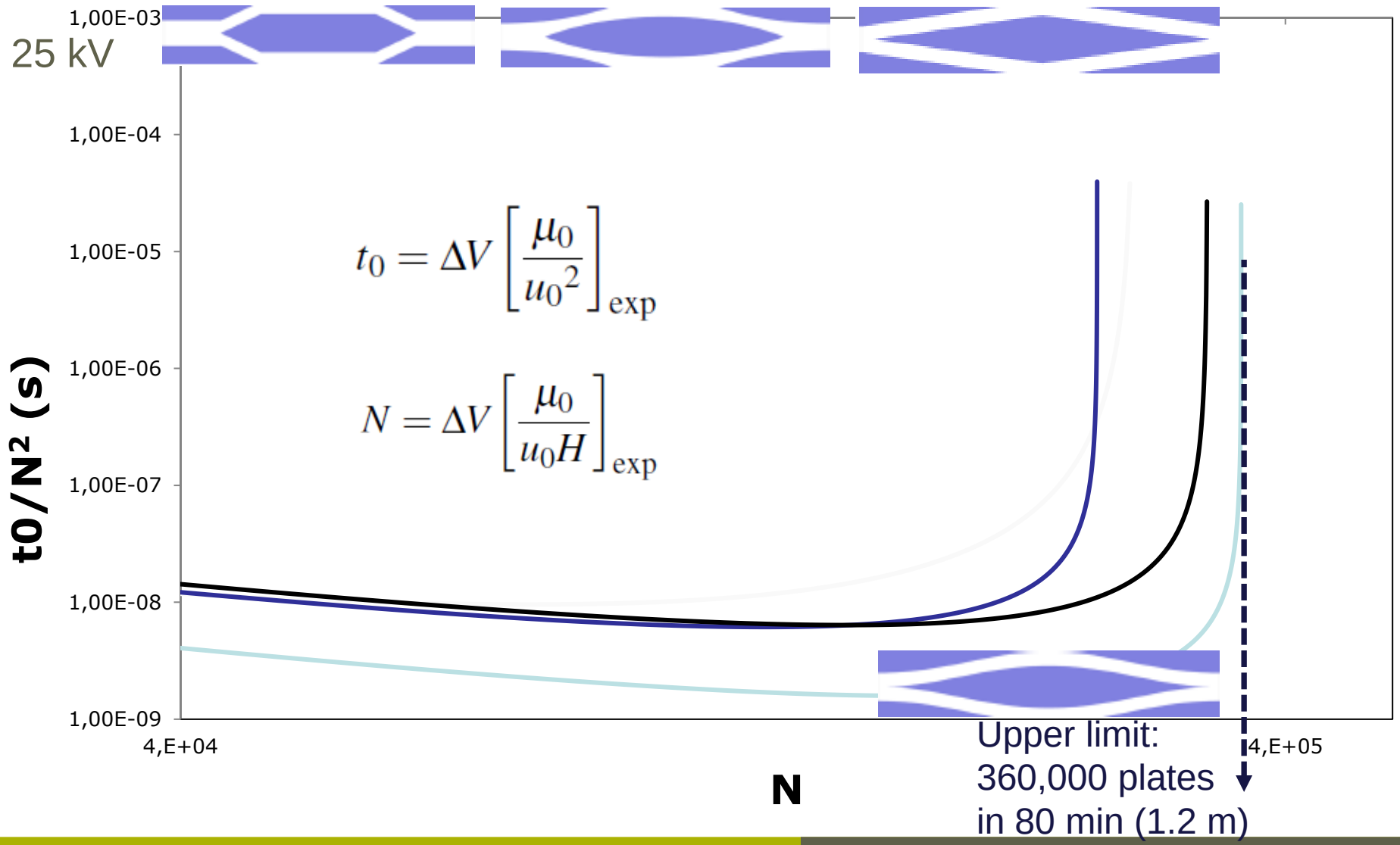

Flow propagation

- Electro-osmotic flow
- Shear-driven
- Pressure

Shear-driven flow

Shear-Driven:

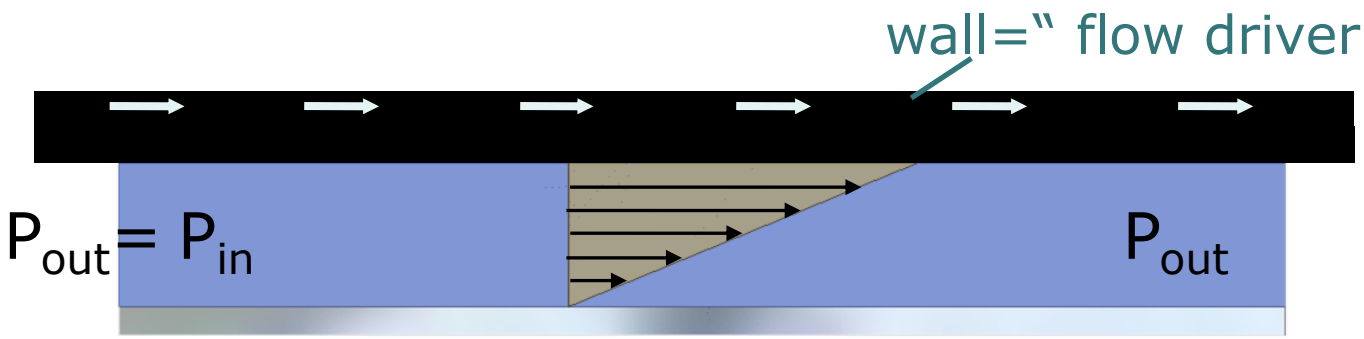

$$u = \frac{u_{moving\,wall}}{2}$$

Pressure-Driven:

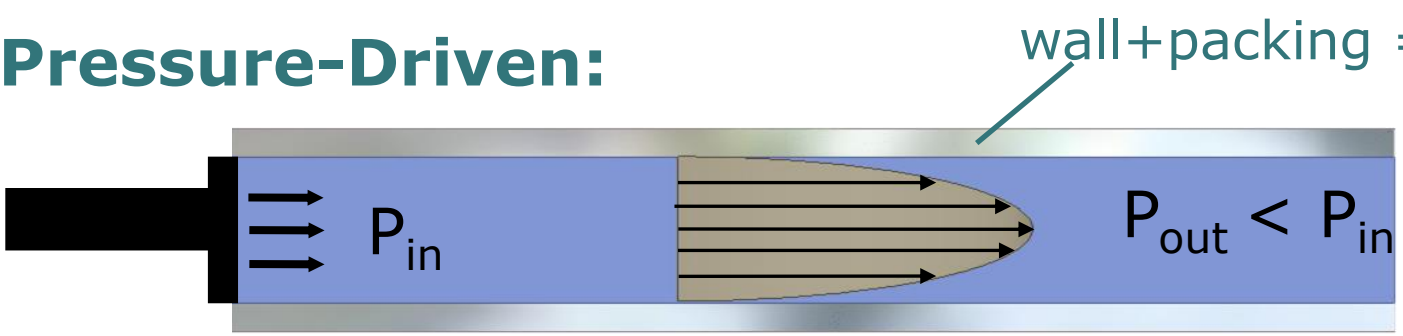

$$u \sim \frac{\Delta P . d_p^2}{L}$$

Flow Driving Force at Channel Inlet

Shear-driven flow

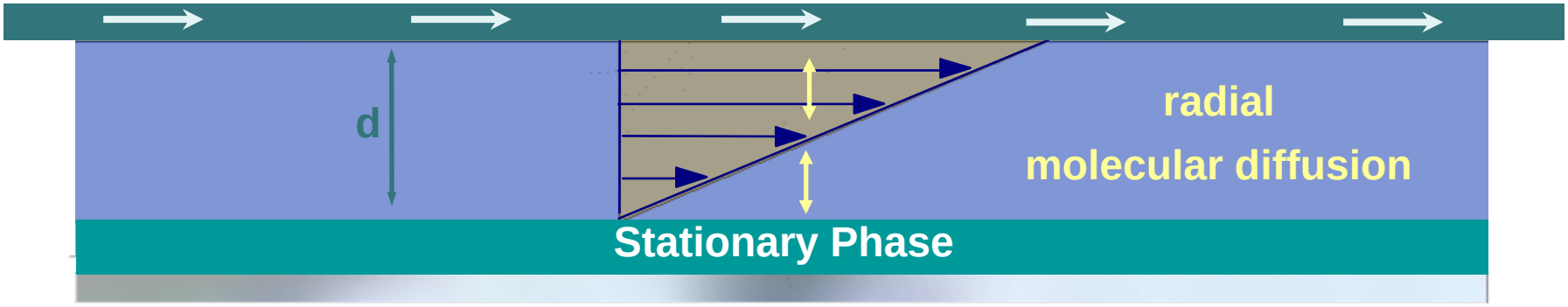

mean velocity: $$u = \frac{u_{moving\,wall}}{2}$$

u and d can be selected independently

No double-layer overlap velocity reduction (cfr. electrically-driven flows)

Desmet, G., Baron, G. (1999). Journal of Chromatography ***855****, 57 – 70.*

Application of shear-driven flows: chromatography

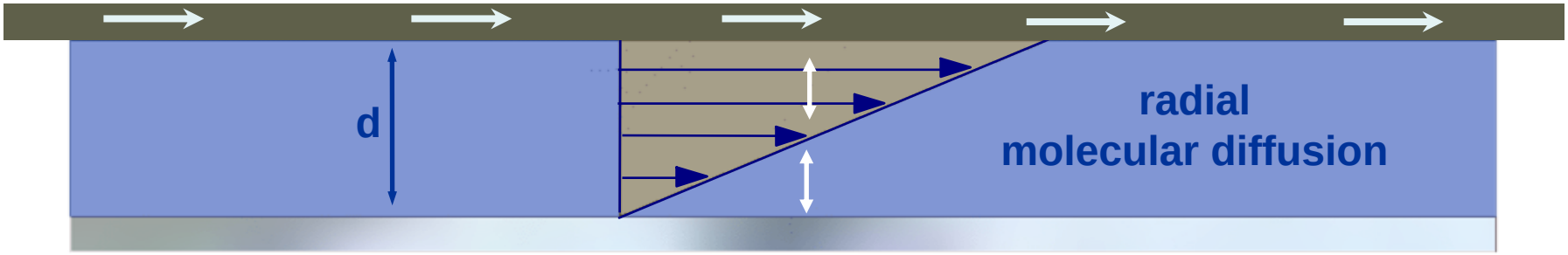

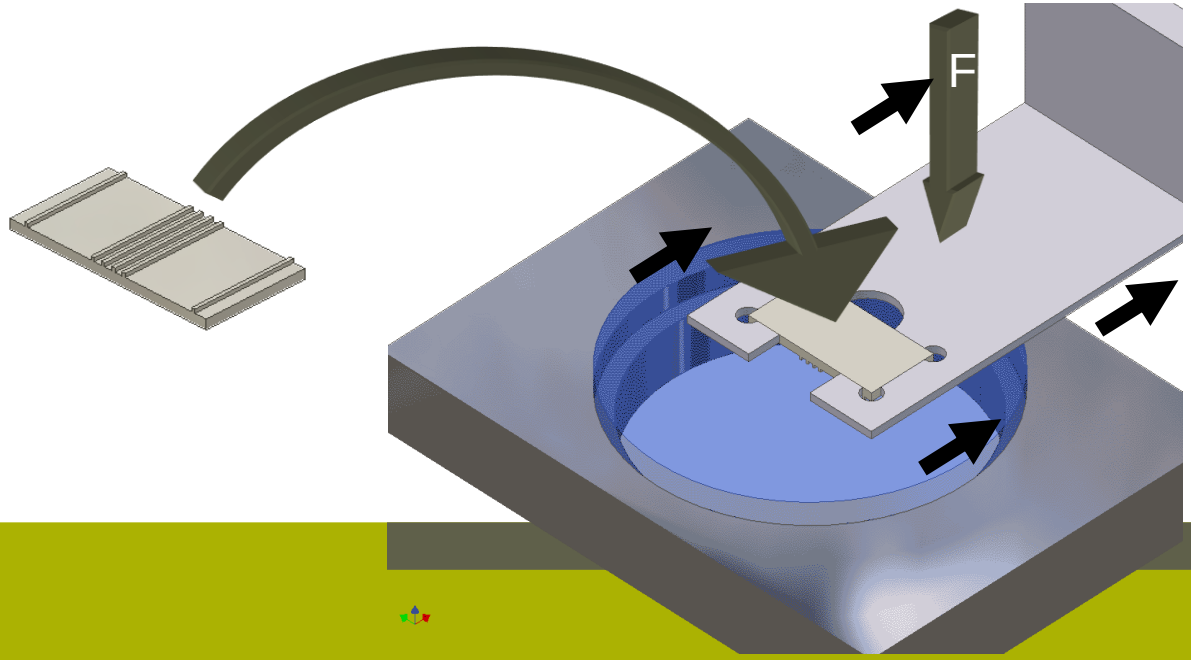

Channel preparation

Silicon platelet (also SiRN, SiO_2, Cr)

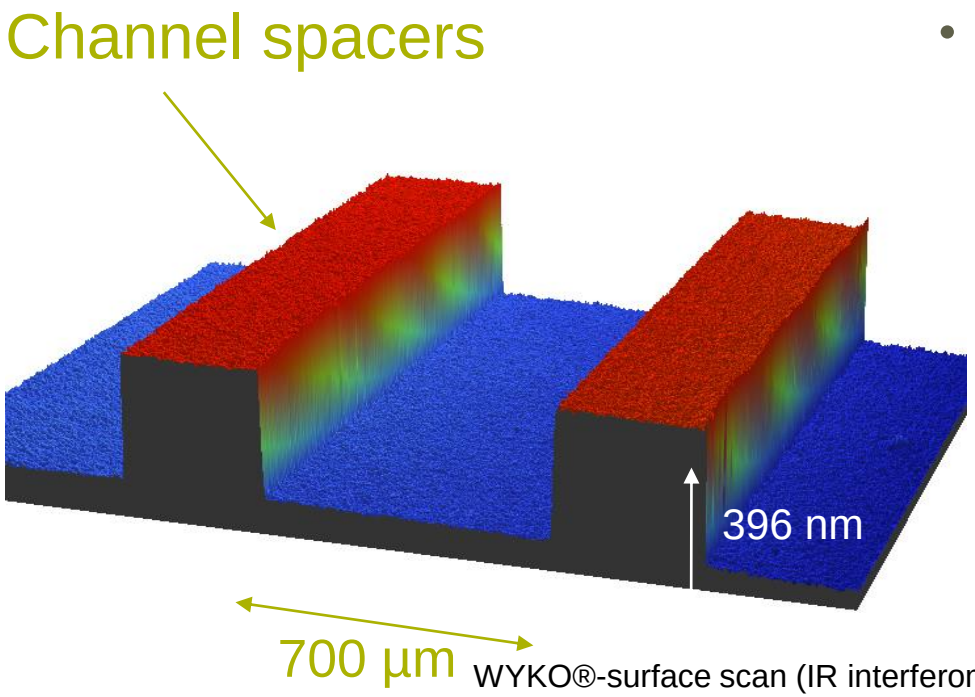

WYKO®-surface scan (IR interferometry)

- Non-etched parts are used as channel spacers in assembled channel
- Pressure load is used to control thickness
- Derivatization of the stationary channel wall with C8 (dimethyloctyl chlorosilane) or C_{18}

Injection procedure

Aris theory: exact velocity profile of secondary importance

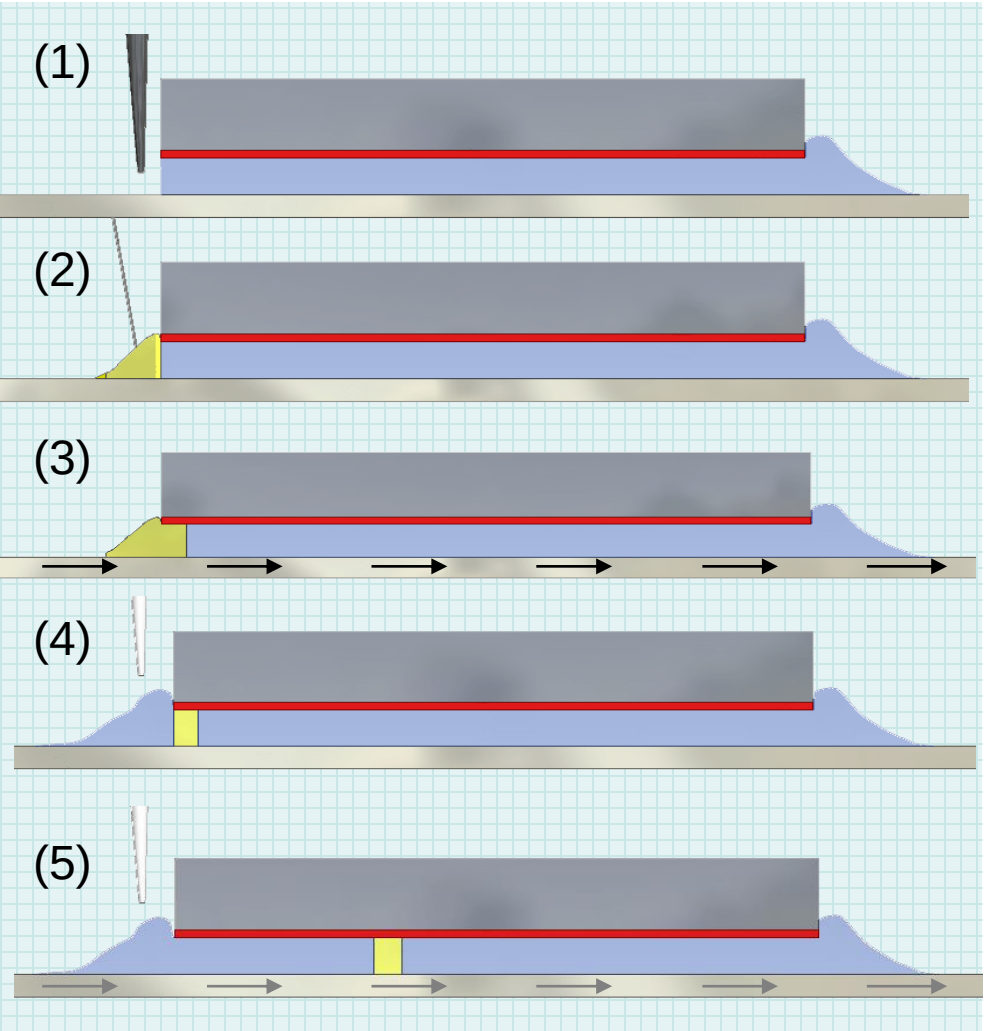

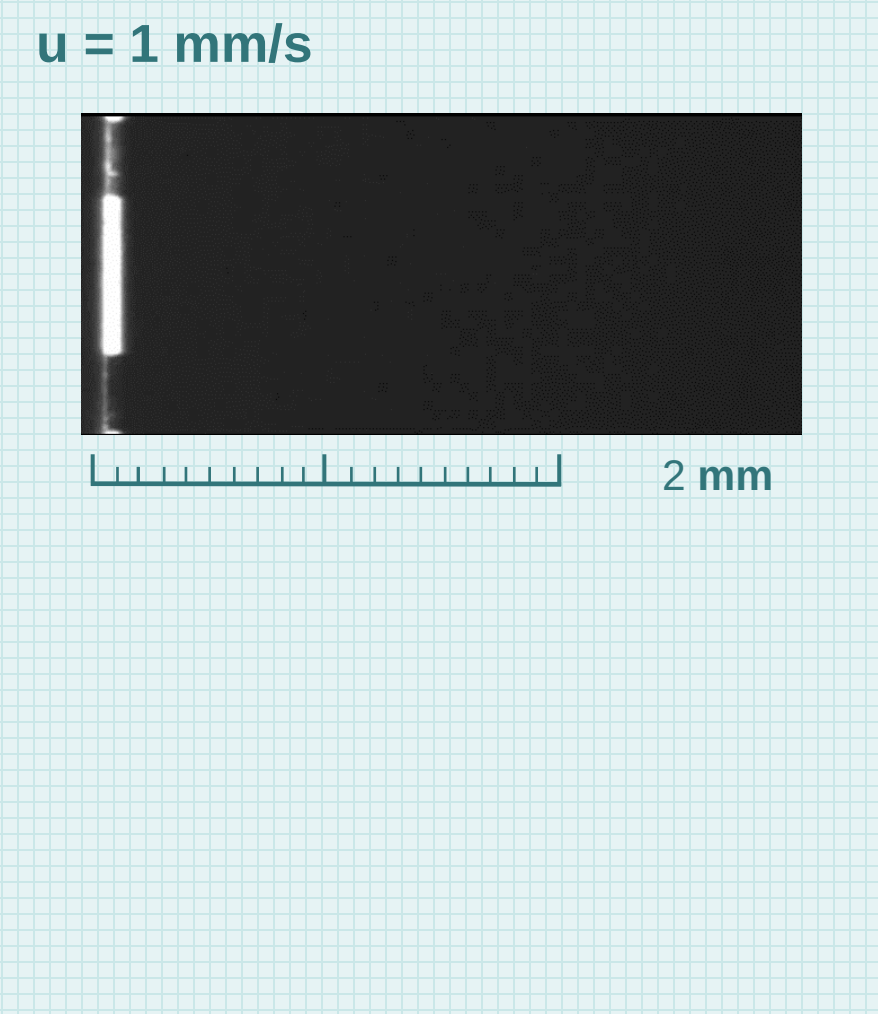

Stationary phase = C8

Mobile phase= 50% methanol

Depth 110 nm

2 cm /s (110nm x 700 µm x 15 mm) equal to 4000 bar if P driven

(separation of 4 coumarin dyes in < 0.1 s)

Size separation of nano-particles

Principle:

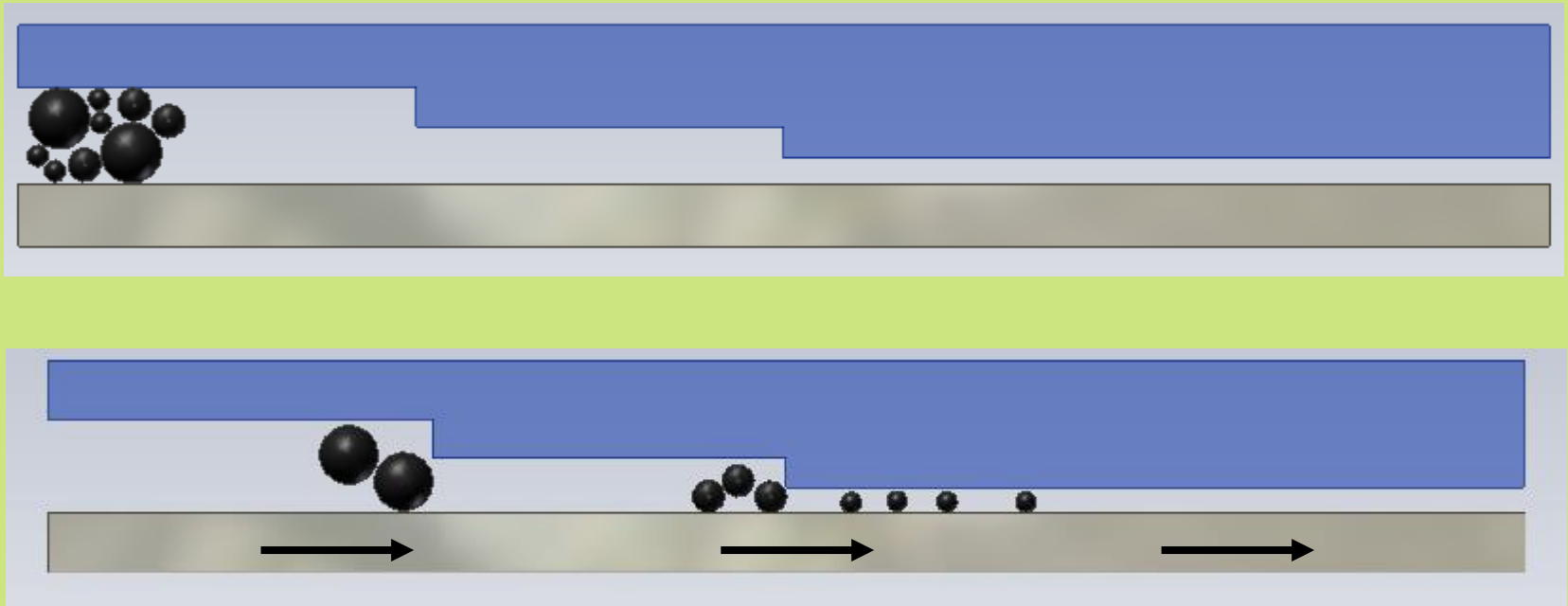

Use particle confinement to induce size-dependent separation
in stepwise tapered channel

Physical separations

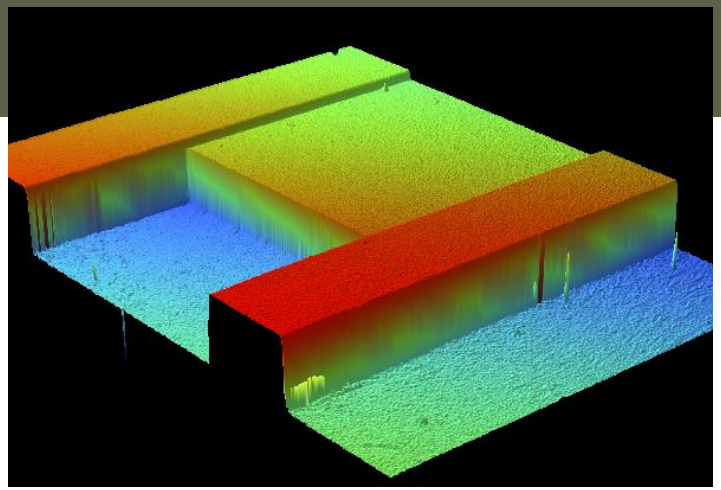

1 μm and 0.5 μm particles in a stepped structure

H=3 μm | H=0.8 μm

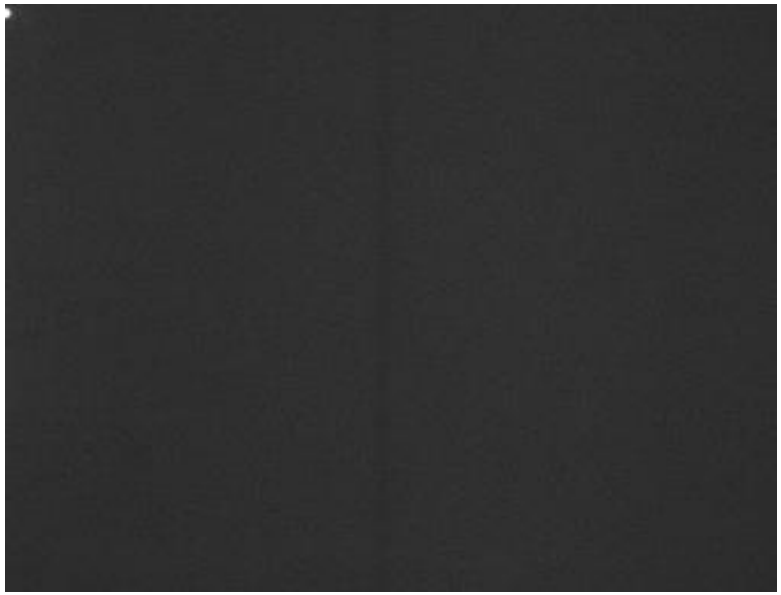

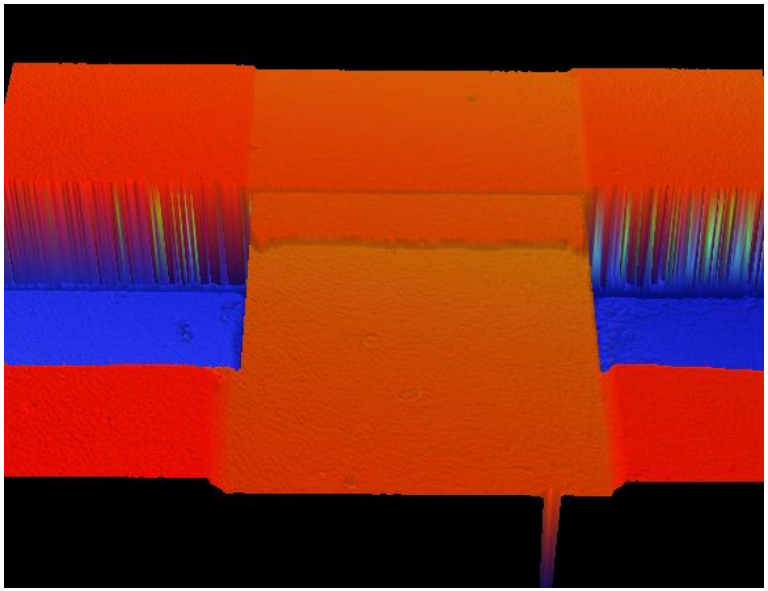

Major hurdle: detection

Detection groove

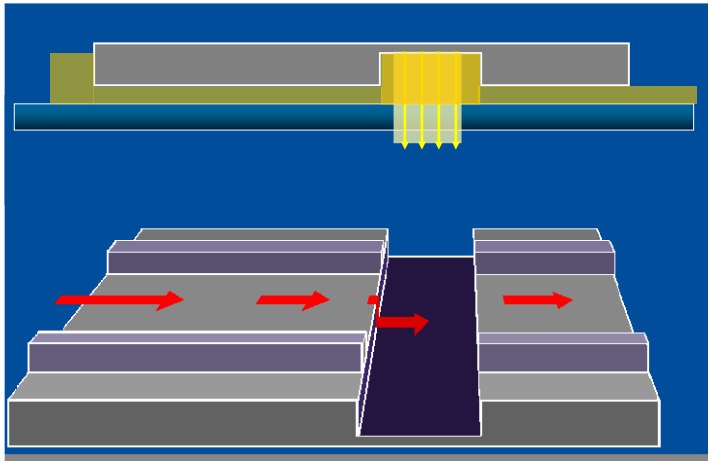

Fundamental problems: statistics (less than 1 molecule/sample), detection

Flow propagation

- Electro-osmotic flow
- Shear-driven
- Pressure

Pressure-driven flow

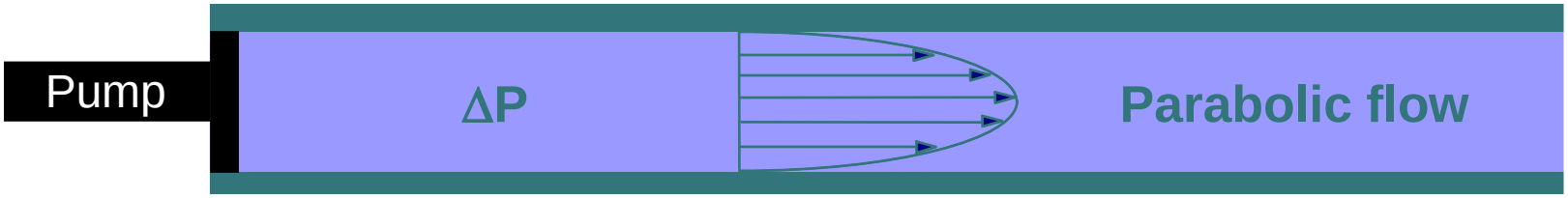

Law of Poiseuille (w>>h):

$$u = \frac{\Delta P_{max}.d^2}{12.\mu.L}$$

u=1 mm/s in L=0.1 m and d=100 nm: 1200 bar needed !

Traditional approach HPLC: packed bed

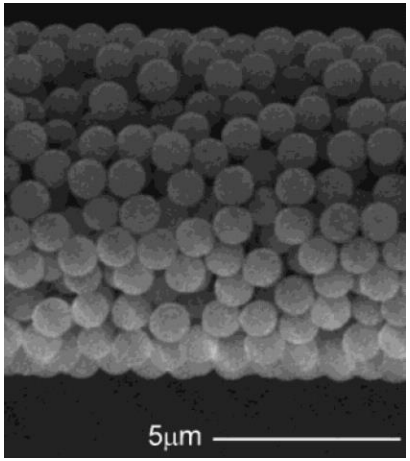

Packed columns
(Jorgenson *et al.*, 2004)

HPLC

(High Performance Liquid Chromatography)

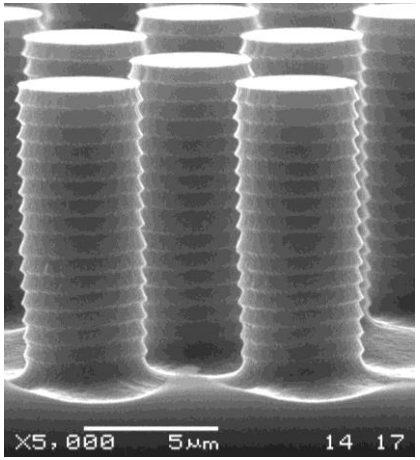

Micro-machined columns

Peak capacity
$P_c \sim 1/4.\ln(k'+1)\sqrt{N}$

Plate height
$H=\Delta\sigma^2/\Delta x \downarrow$

$\cancel{A = 2\lambda d_p}$

- More homogeneous packing: h↓ (2x)
- Channel dimensions can be chosen independent of the size and shape of the support structures (lower flow resistance): Φ↓ (2x) $t_{sep} \sim h^2.\Phi$

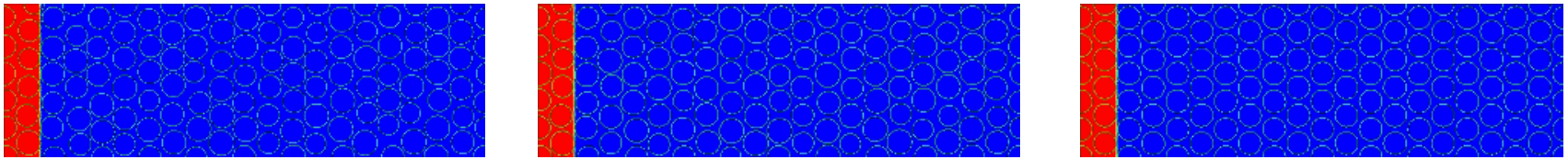

disorder order

Flow resistance

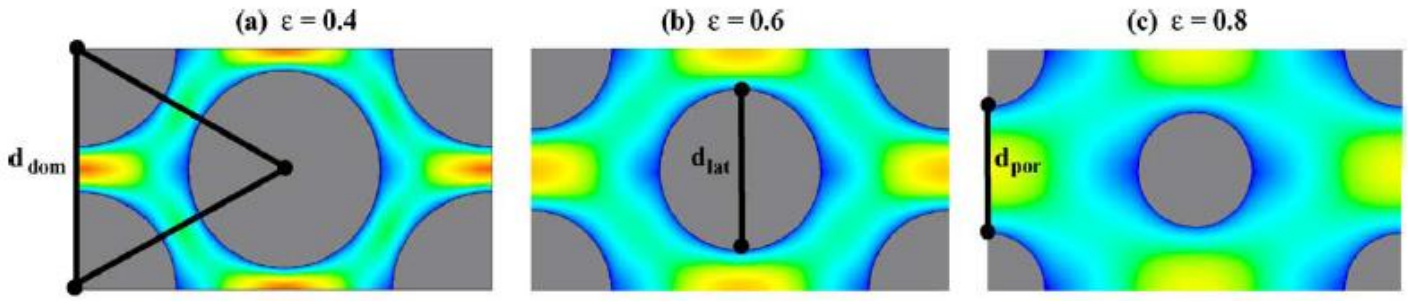

Φ=274 Φ=121 Φ=56

Packed bed (ε=0.4): flow resistance Φ=405

Permeability: $K_v = u.\eta.L/\Delta P$

Reduced flow resistance $\Phi = d_p^2/K_v$

Packed bed (ε=0.4): Φ=405

Gzil *et al.*, Anal. Chem., 2004, 1073, 43

Fabrication

S:sample
MP: mobile phase

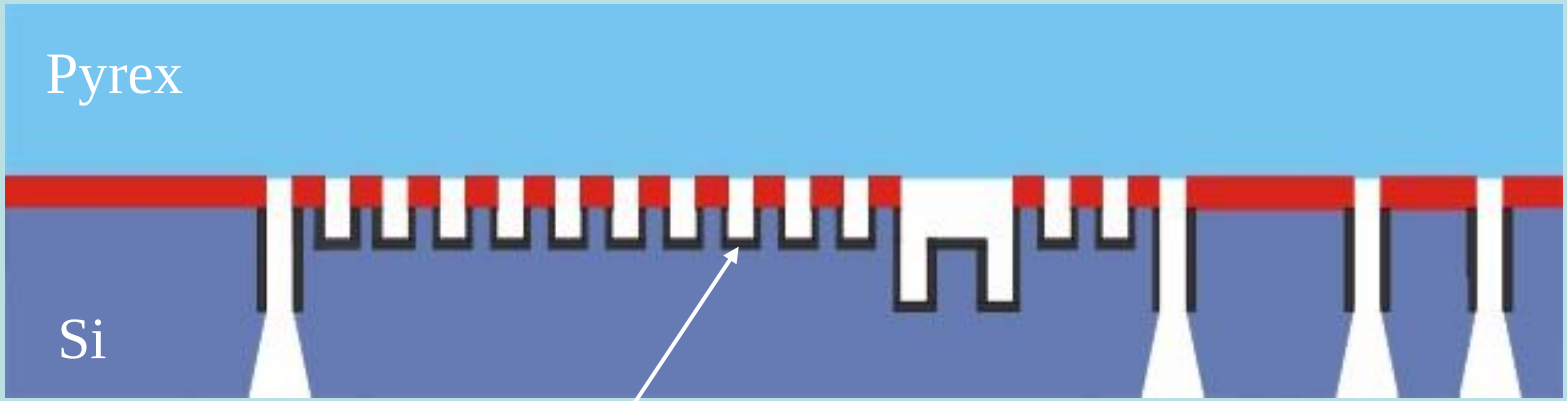

Porous Si

MP out

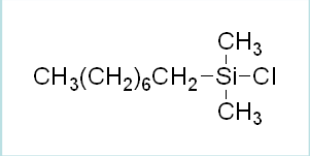

S out S in MP in

Coating procedure: 5 % octyldimethylchlorosilane in toluene
(5 %, 5 µl/min, 4 d)

On-chip injection and detection

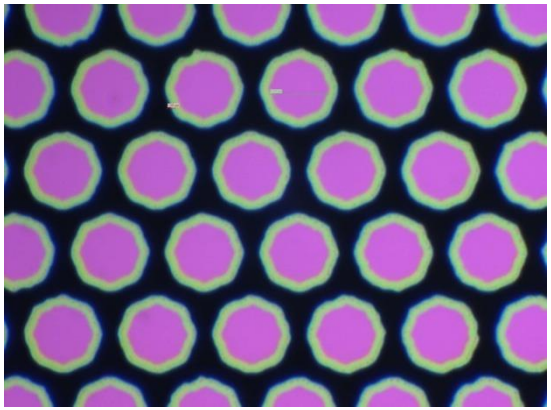

10 µm pillars, void fraction of 40 %

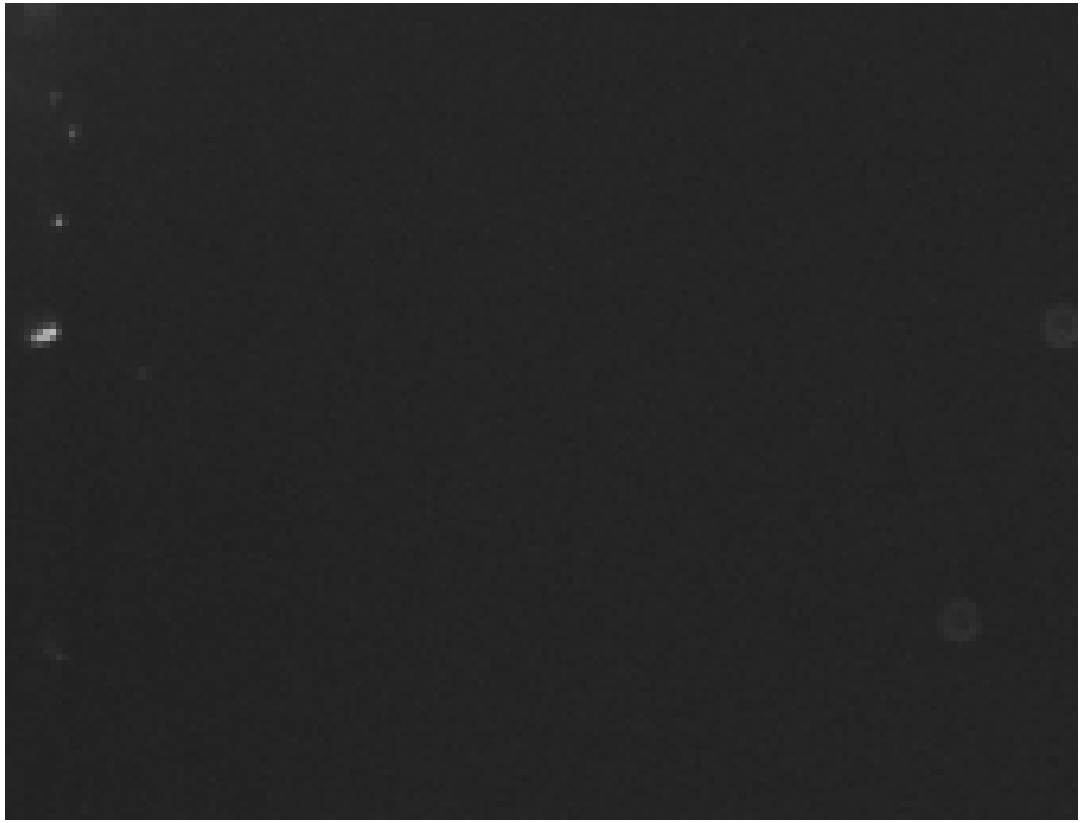

60/40 MeOH/$H_2$0, u=0.23 mm/s, pH 3, C440, C450, C460, C480

Porous shell pillars

Typical data available in the literature for packed columns

(N. Wu,, *et al.*, J. Chromatogr. A, 2006, 1131, 142)

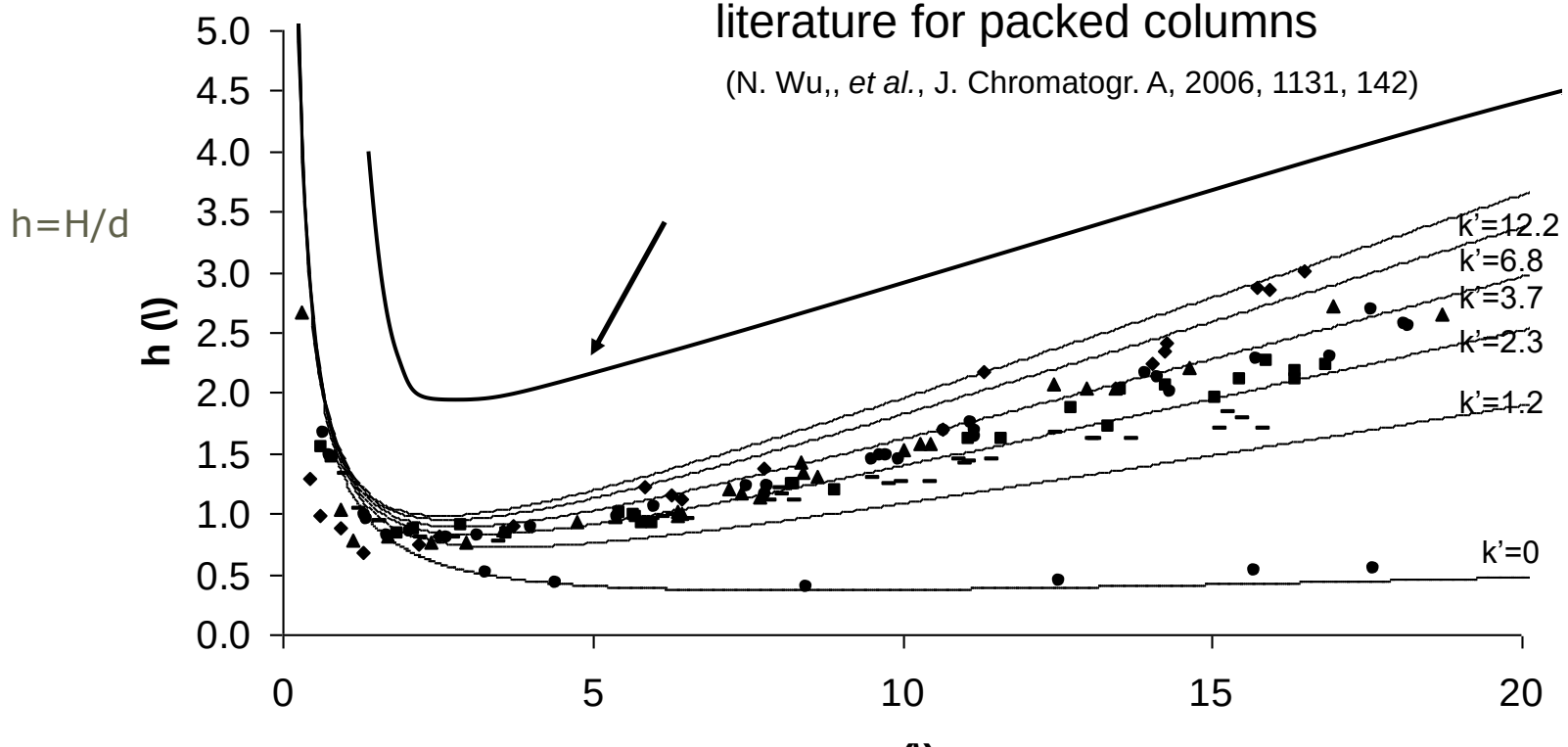

$t_{sep} \sim h^2.\Phi$ with $\Phi = d_p^2/K_v$

Porous shell pillars with C8-coating, C480 in water/methanol mixtures (d_p=10 µm, d_{shell}=1µm)

De Malsche *et al.*, Anal. Chem., 2008, 80, 5391

Imprinting (cyclo-olefin copolymer)

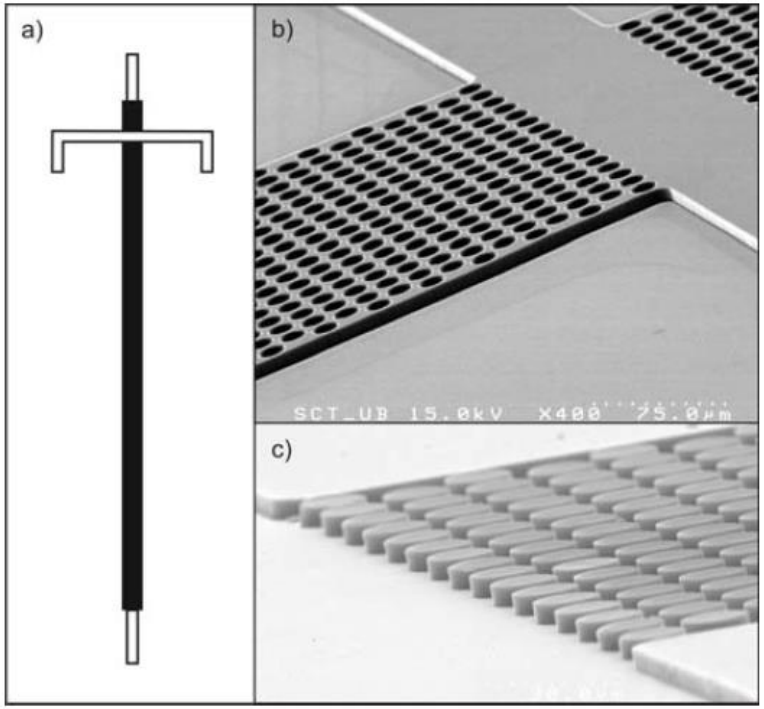

imprint

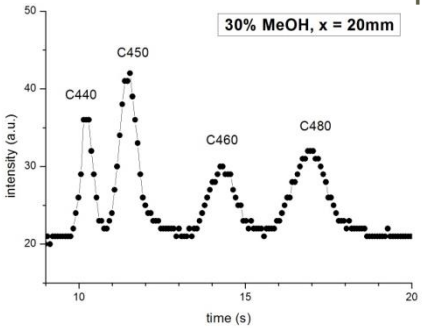

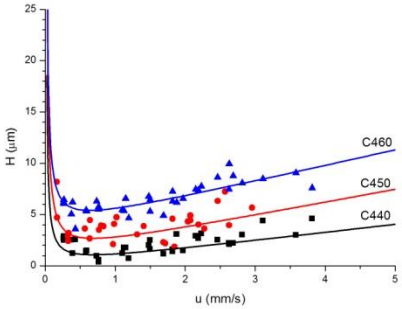

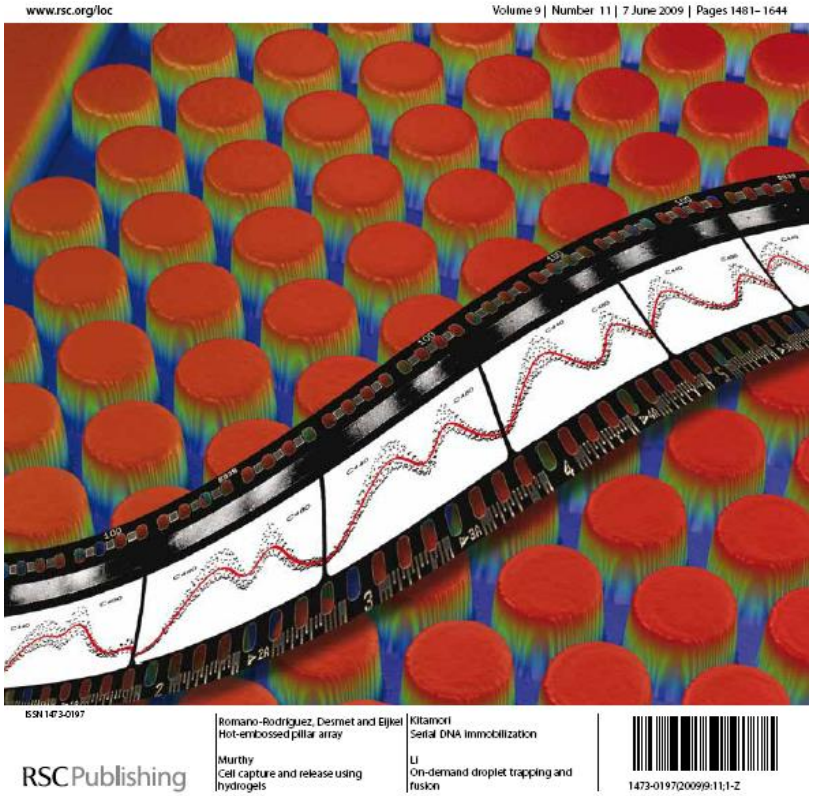

Illa, X., De Malsche, W., Bomer, J., Gardeniers, H., Eijkel, J., Morante, J.R., Romano-Rodriguez and Desmet, G. (2009), *An Array of Ordered Pillars with Retentive Properties for Pressure-driven Liquid Chromatography Fabricated Directly from an Unmodified Cyclo-olefin Copolymer*, Lab Chip, 9, 1511-1516 -

Operating at high N: long channel length required

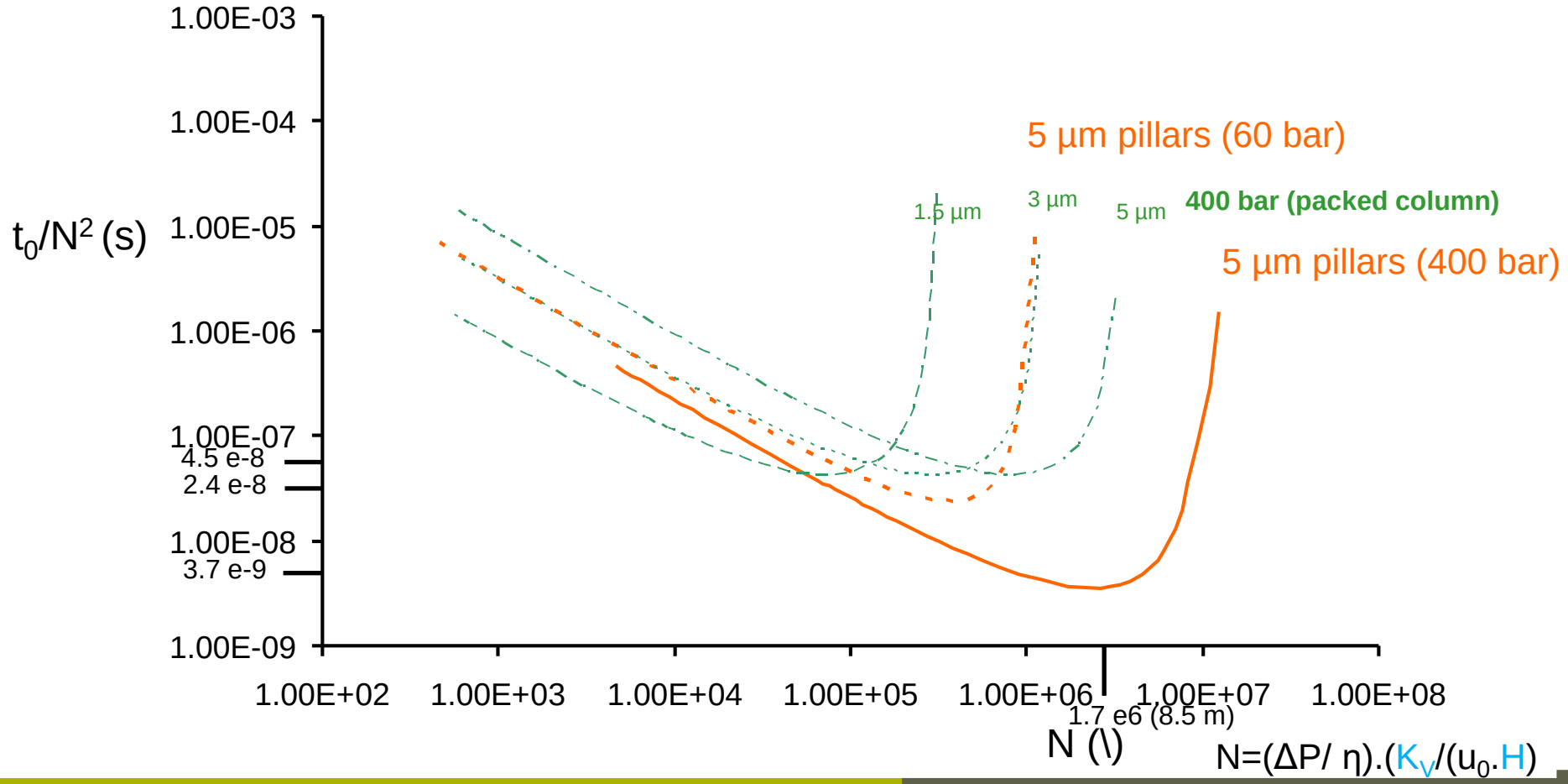

Long channels

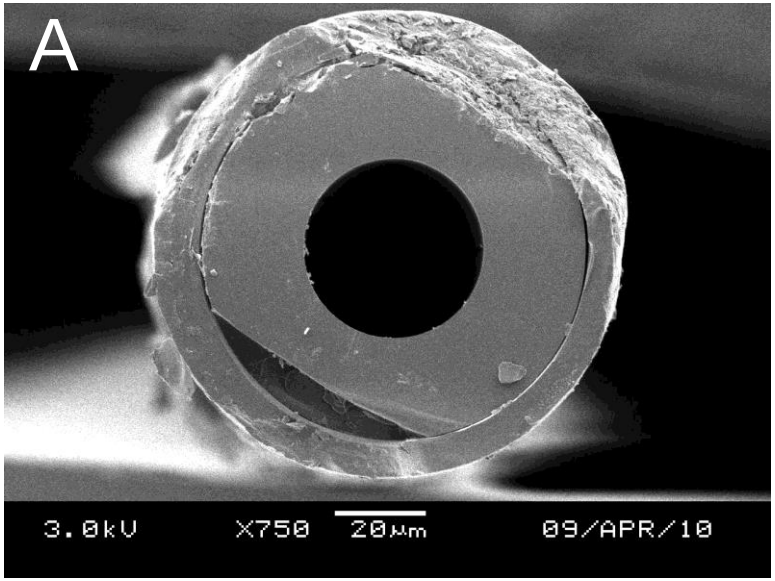

A: Capillaries as feed
B: Liquid distributor
C: Multiple lanes

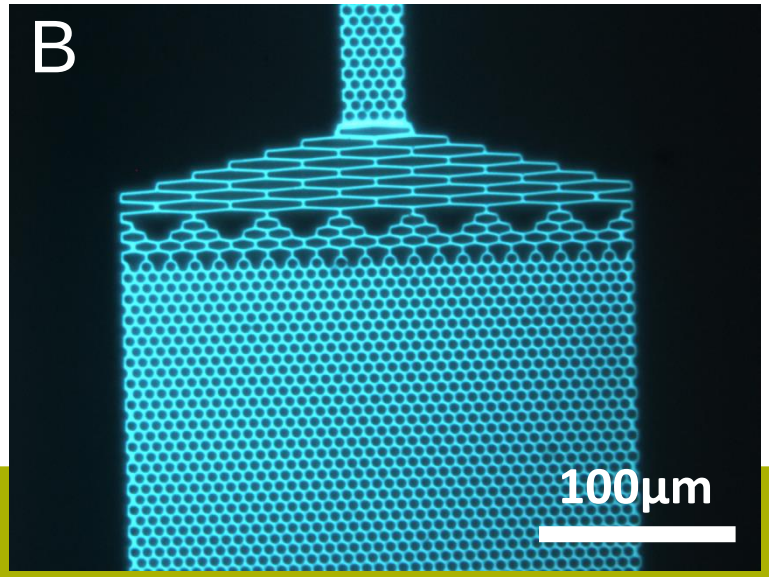

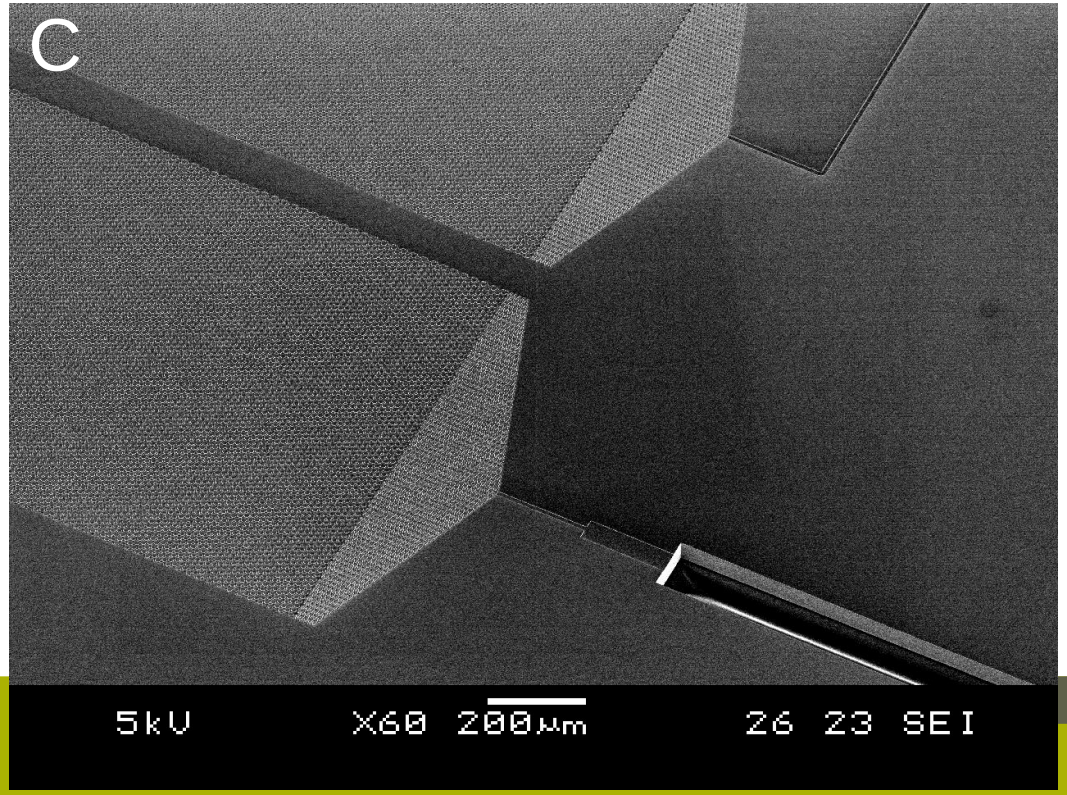

Nanoflow instrument

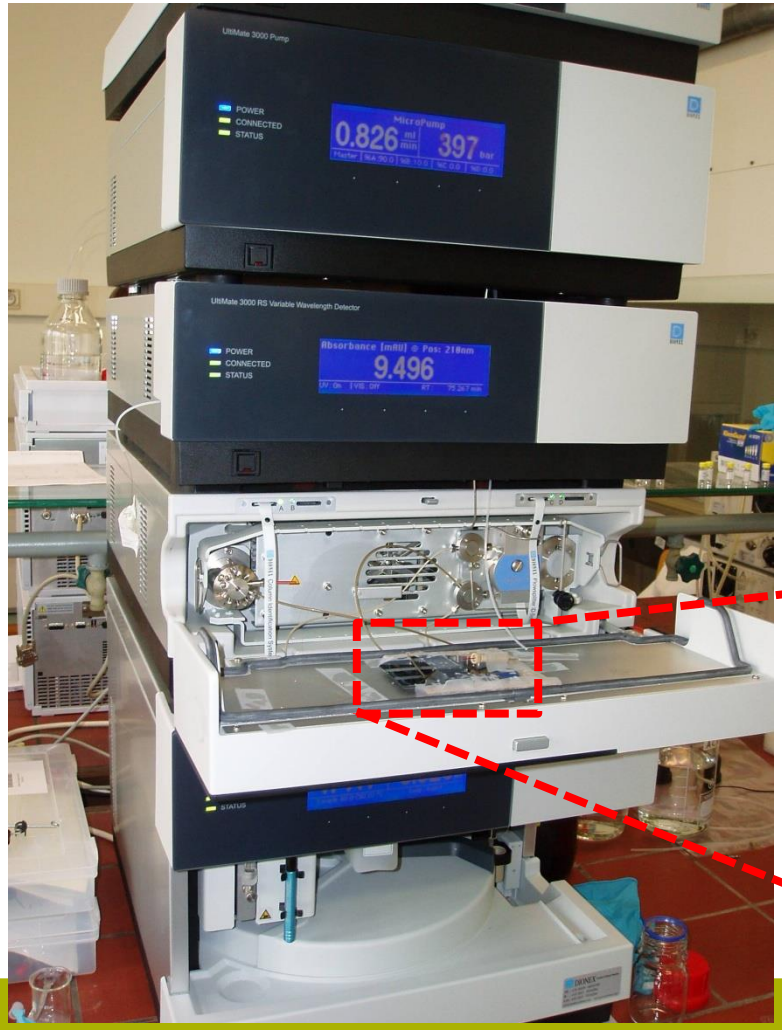

Commercial Nanoflow HPLC pump (Dionex)

Injection volume: 15 nl -1 µl

UV absorption (λ=210-338 nm)
detection cell 2 nl

Transition of 10 µm to 1 mm

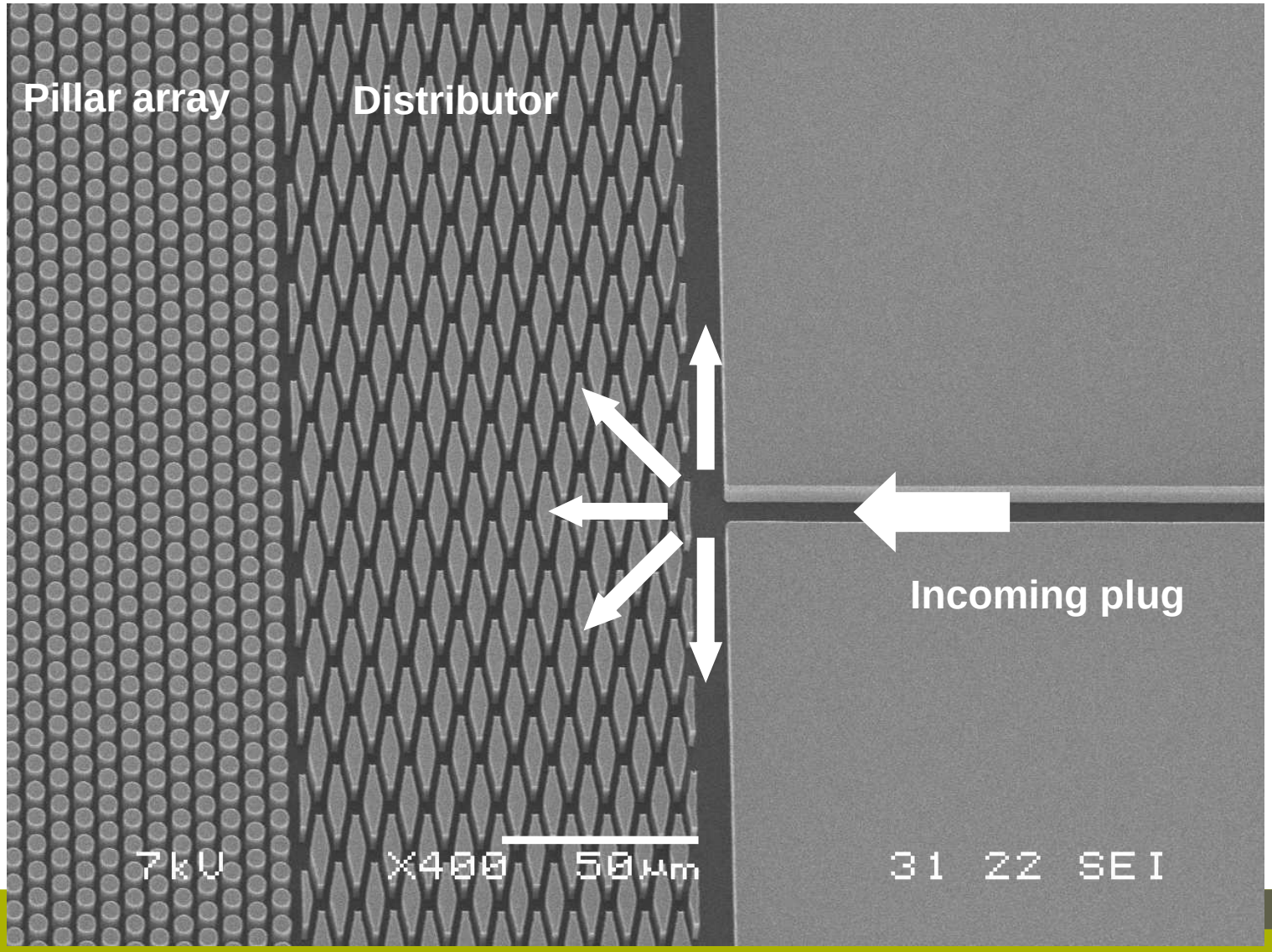

Vangelooven *et al.*, Anal. Chem., 2009, 81, 943.

Reducing dimensions

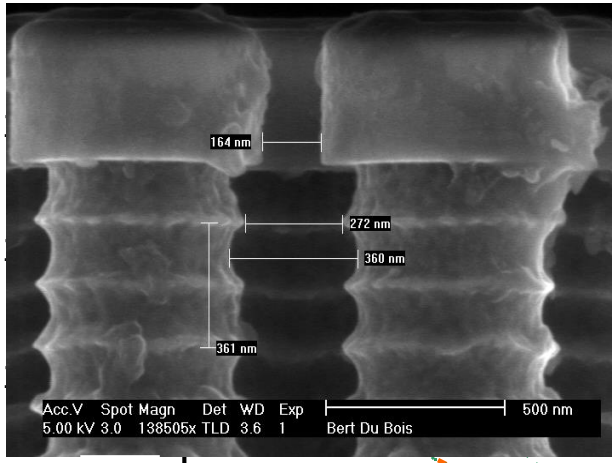

Deep UV litho required: cooperation with Interuniversity Micro-Electronics Center (Imec, Leuven, Belgium)

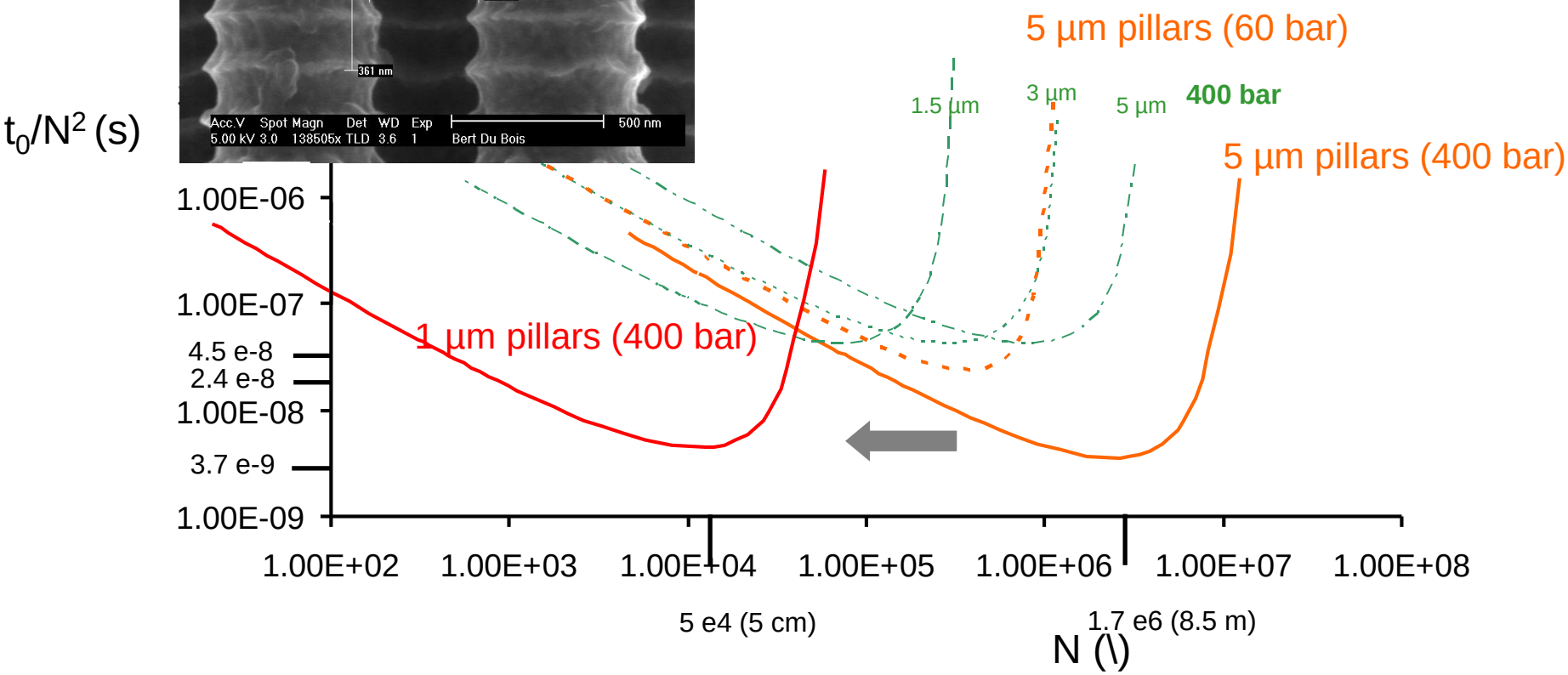

$N_{opt} \sim d_p^2$

$d_p \downarrow$ Dimensionless van Deemter curves

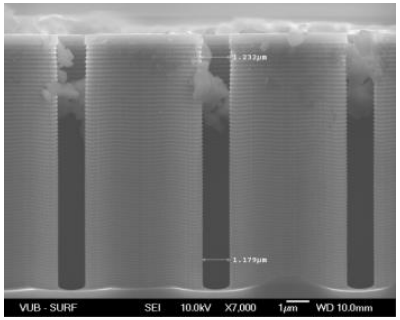

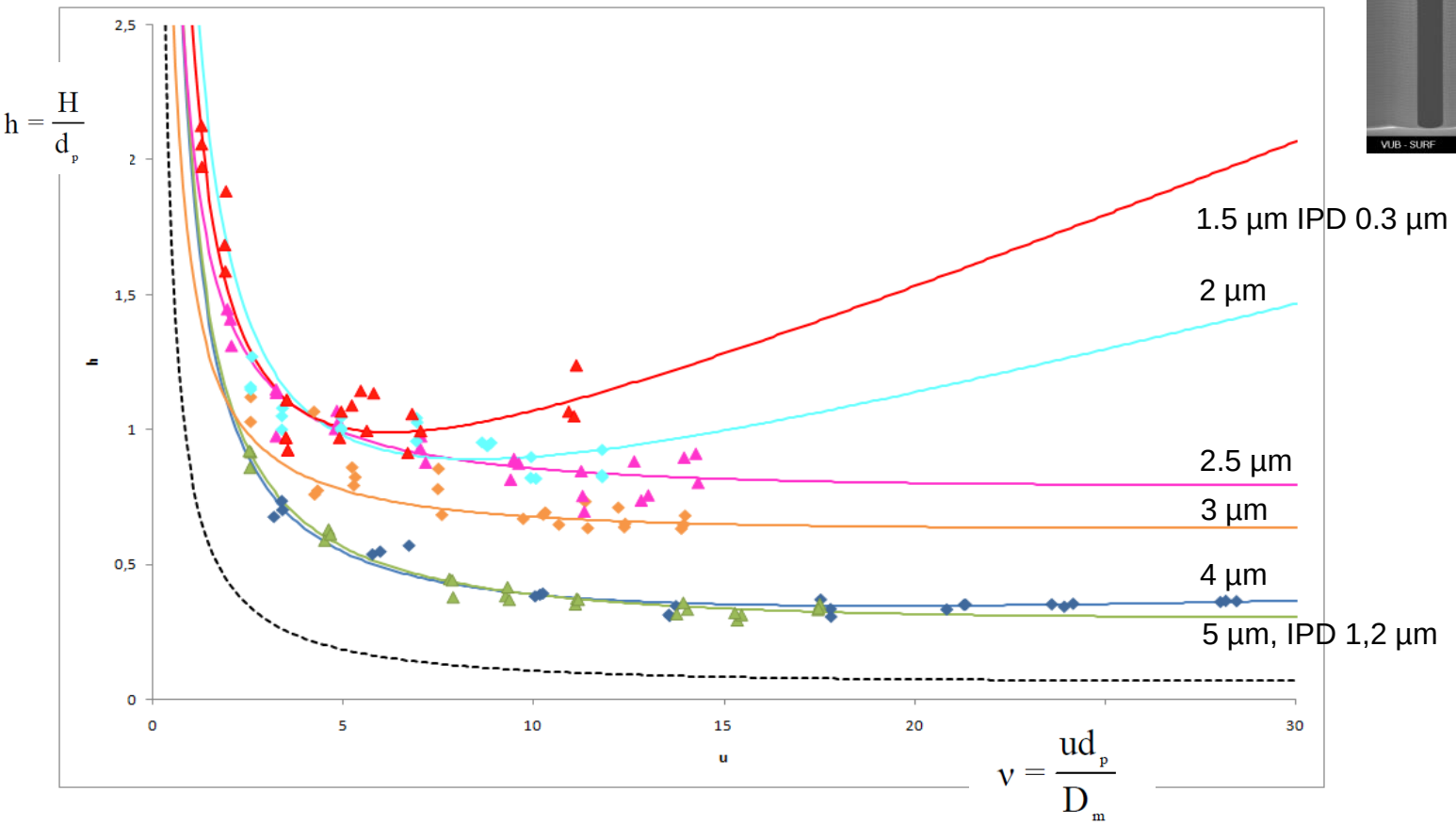

Aspect ratio (depth/spacing) ↑→ h ↗

→ decrease depth (impact on detector sensitivity requirements)

Sidewall effects h ↗

Non-verticality: dispersion source

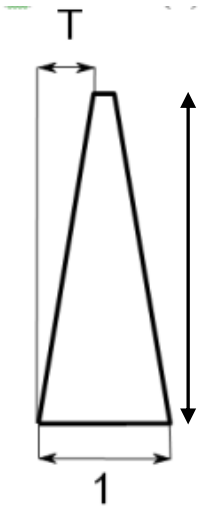

$$h = \frac{2}{v} + 2 \cdot \kappa_{\text{Aris}} \cdot v$$

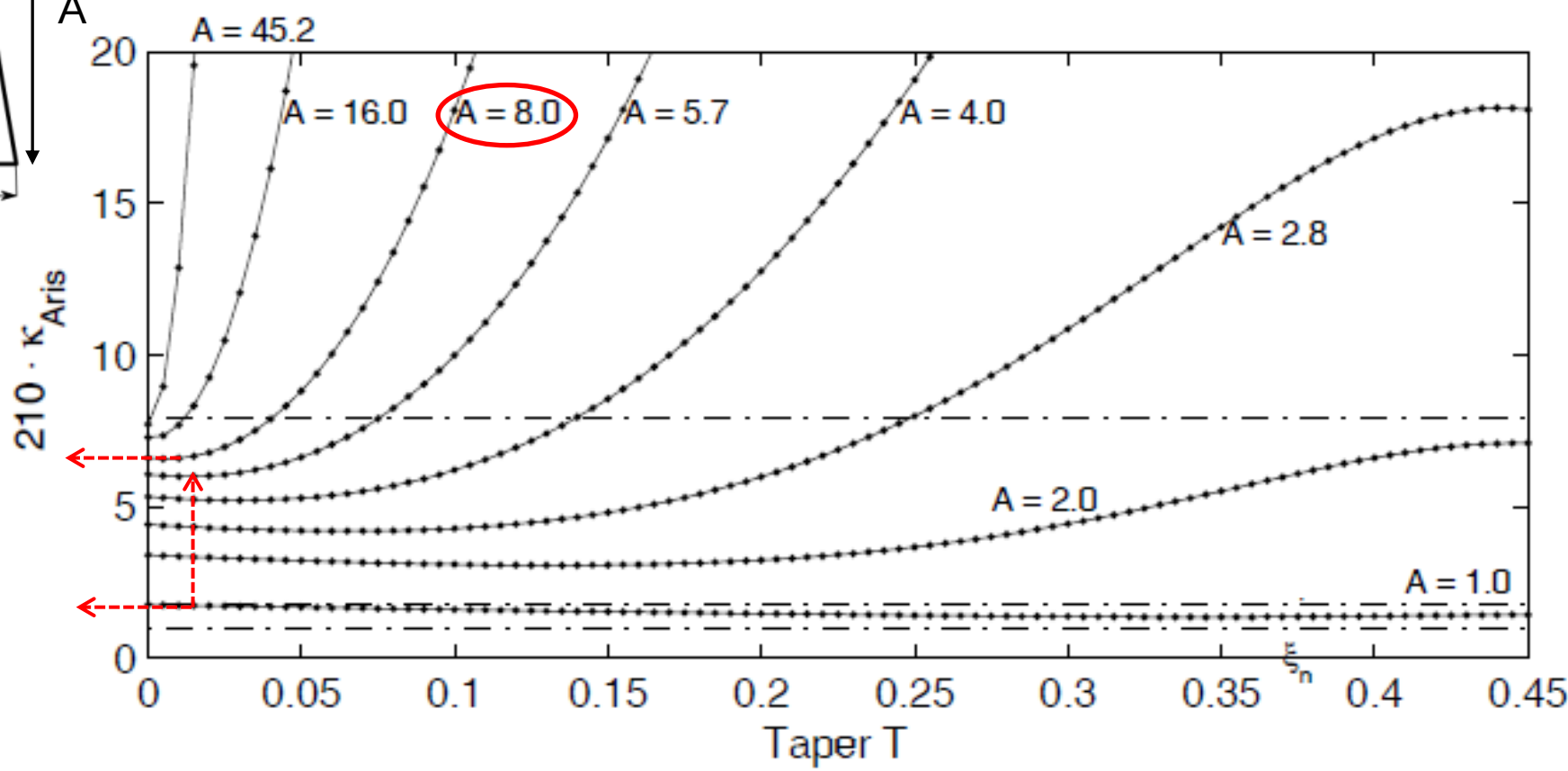

I-shape

$$h = \frac{2}{\nu} + 2 \cdot \kappa_{\text{Aris}} \cdot \nu$$

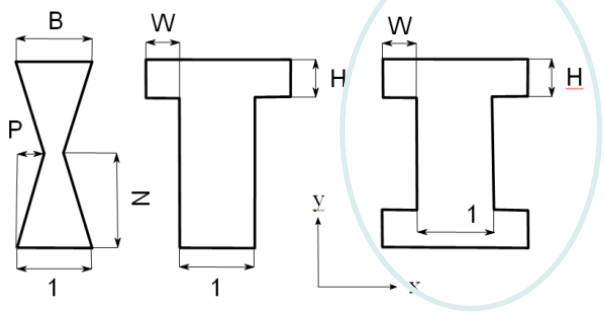

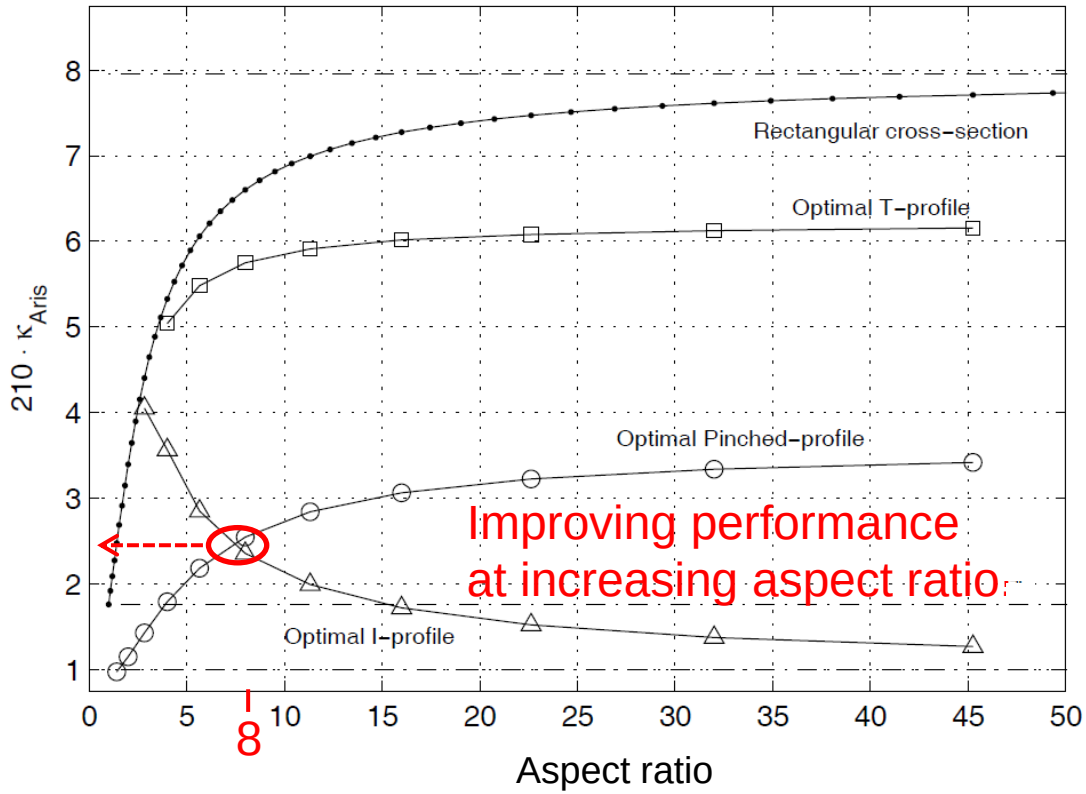

Callewaert, M., De Malsche, W., Thienpont, H., Ottevaere, H., Desmet, G. (2014), Journal of Chromatography A, 1368, 70-81

Sidewall effect

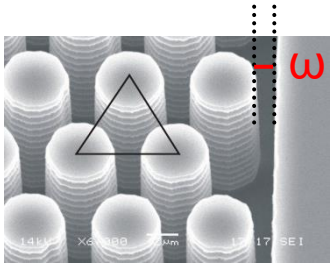

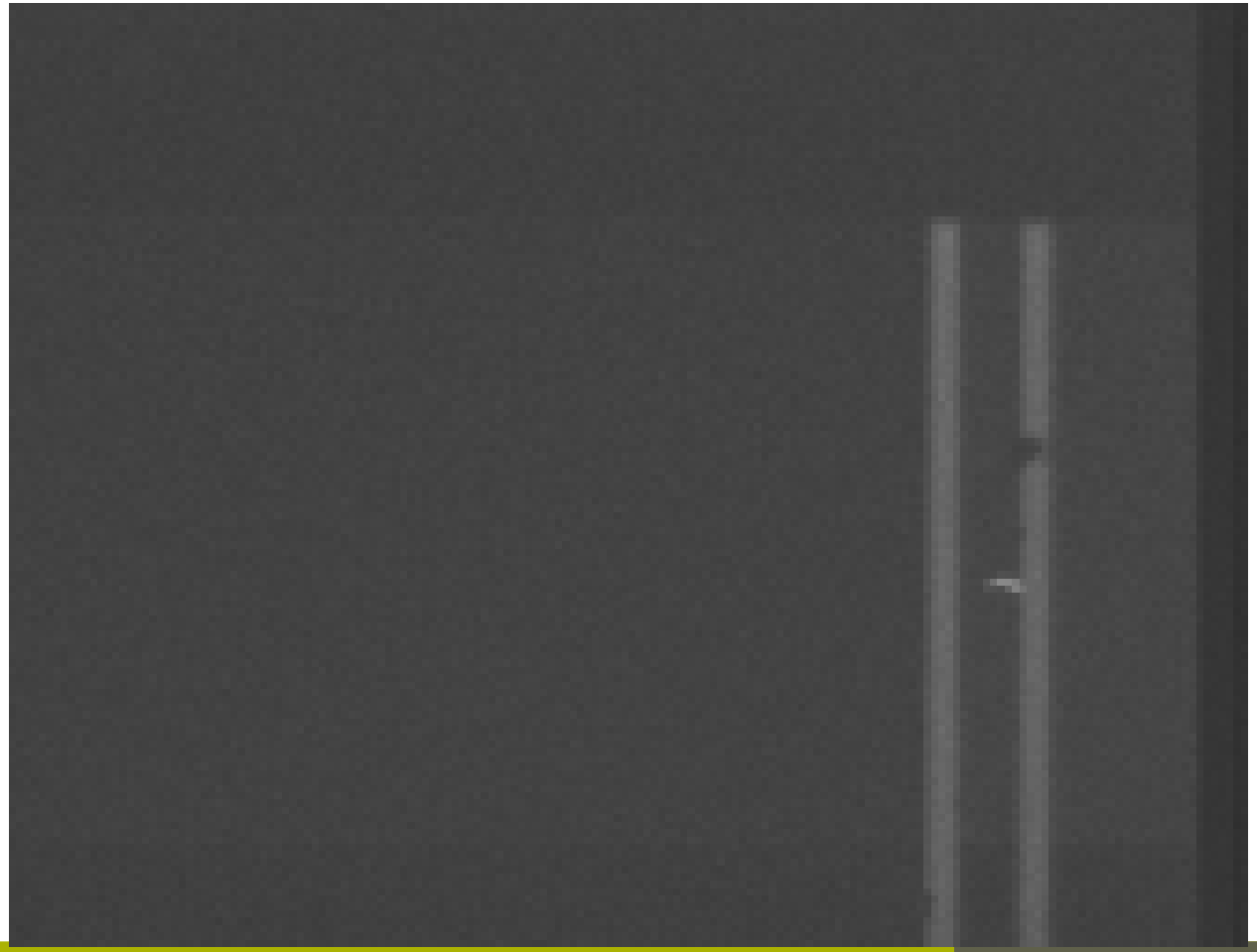

Spacing 1.5 µm
ω_{mag}= 0.75 µm
ω_{eff}= 1.2 µm

C480 in MeOH (1mM)

Sidewall effect

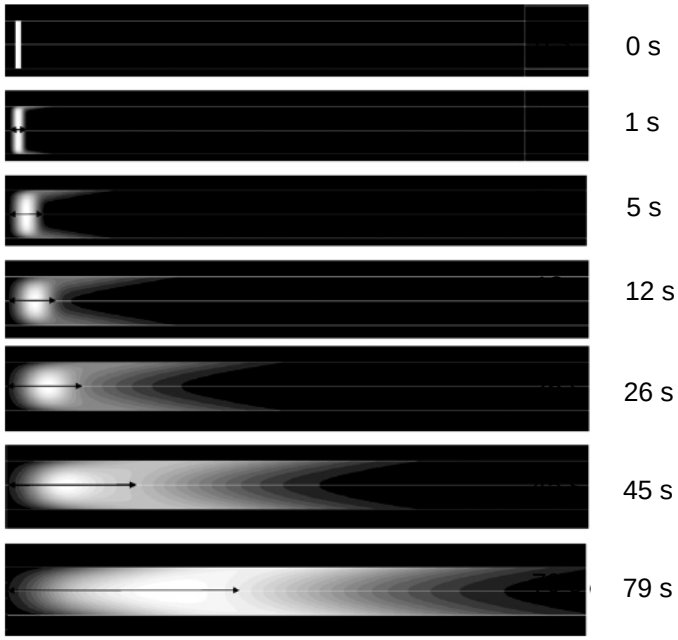

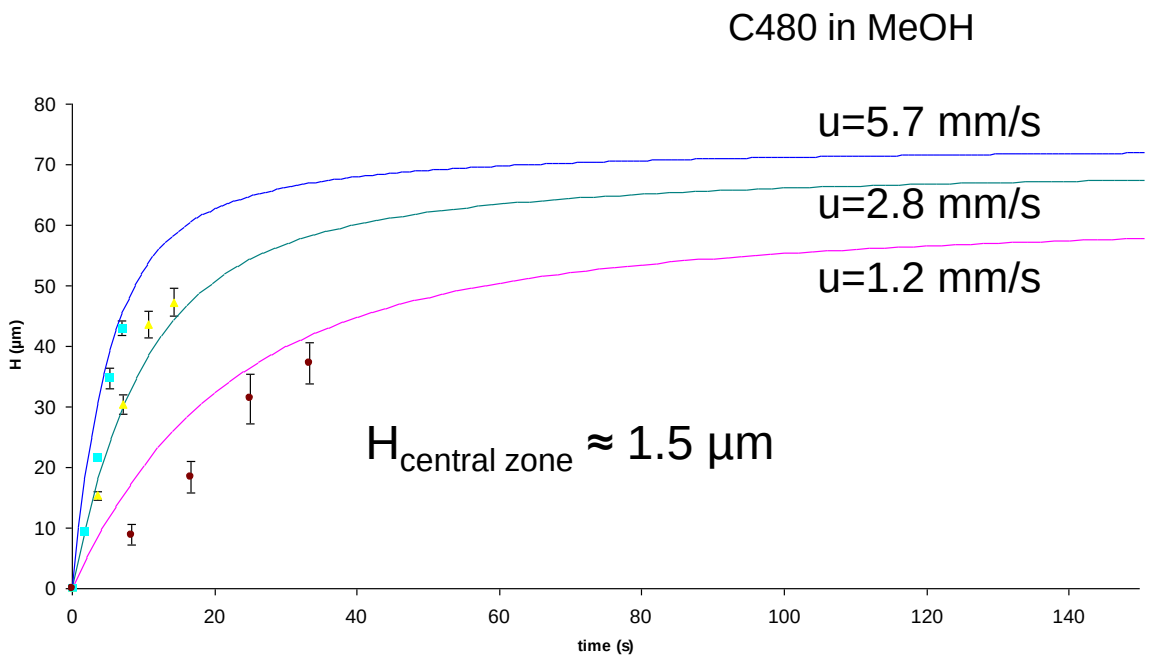

$D_{rad}=2.10^{-9}$ m^2/s, 1 mm wide channel, $u_w/u_c=1.5$, $\delta=5$ µm

Fitted on model based on 5 µm sidewall zone with different velocity as compared to central region (ratio is 1.5)

Model: K. Broeckhoven *et al.*, J. Chromatogr. A , 2007, 1172, 25

Sidewall effects REPs

CYLINDRICAL
HEXAGONAL

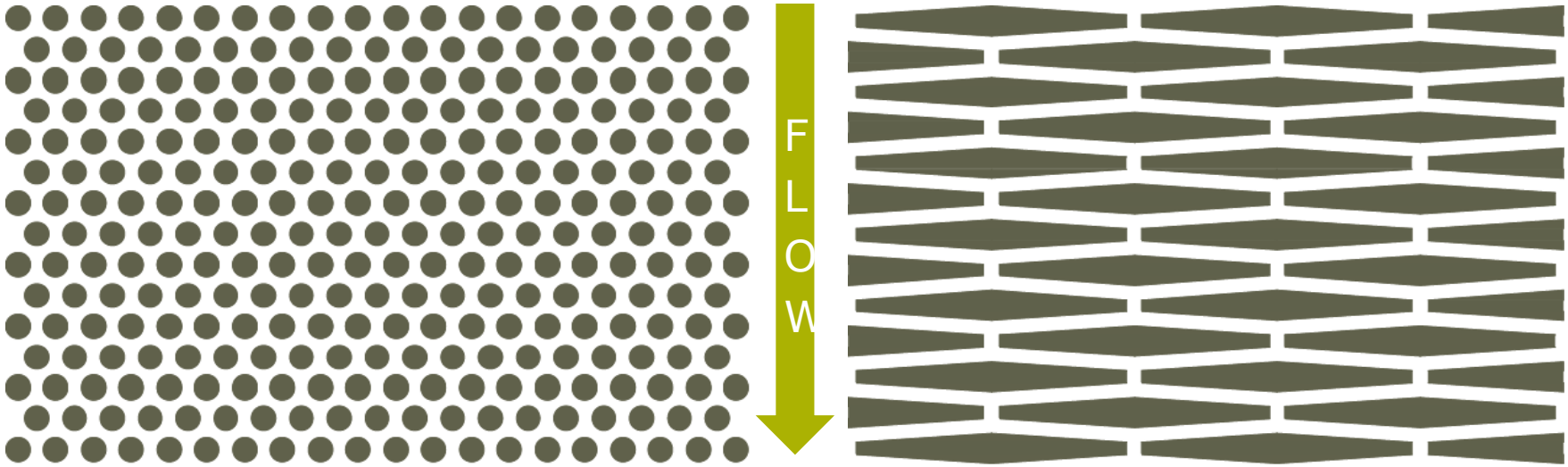

↓ axial dispersion

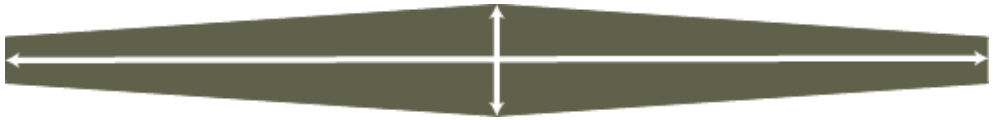

Aspect ratio AR = radial length /axial length of pillar

Sidewall effects REPs

Critical parameter = minimal sidewall distance

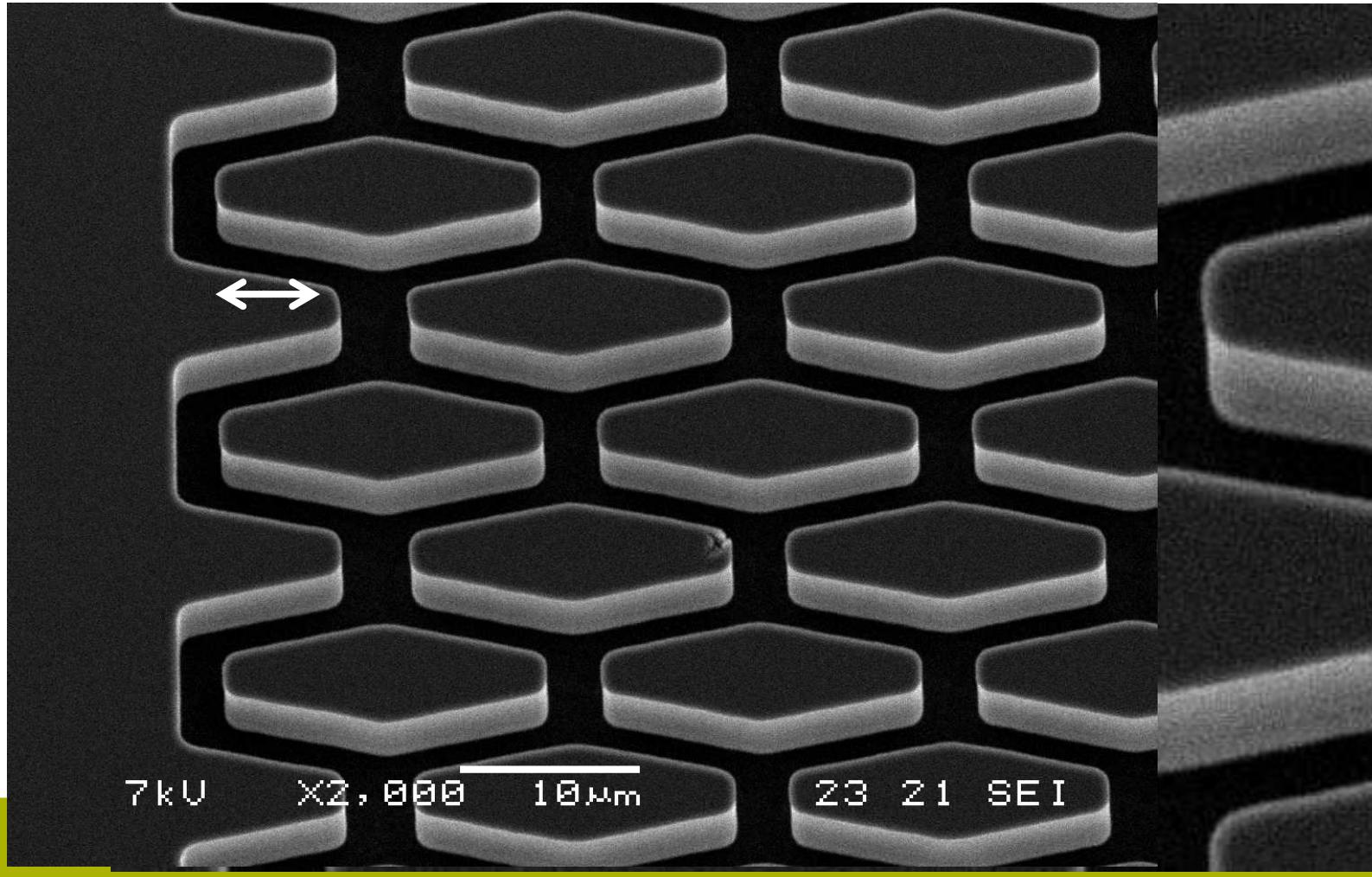

Sidewall effects REPs

Inter-pillar distance: 3 µm

AR 3 Hexagons
6 µm long
18 µm wide

AR 9 Hexagons
6 µm long
54 µm wide

Sidewall distances: **2.0 / 2.6 µm**

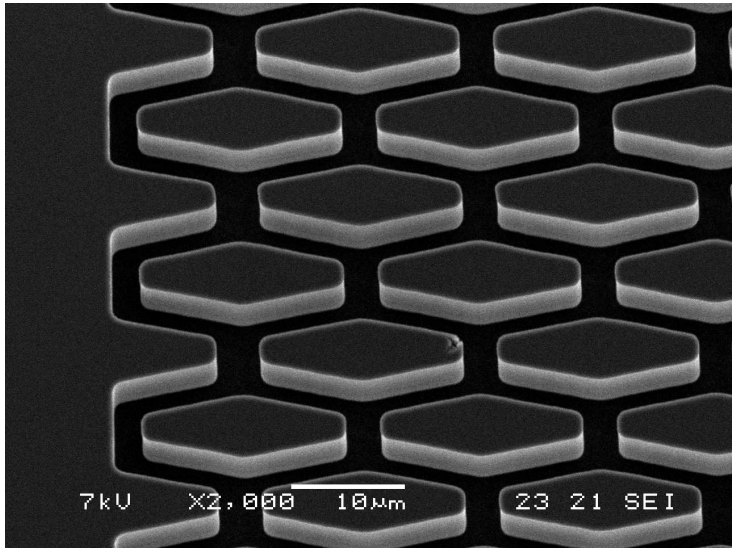

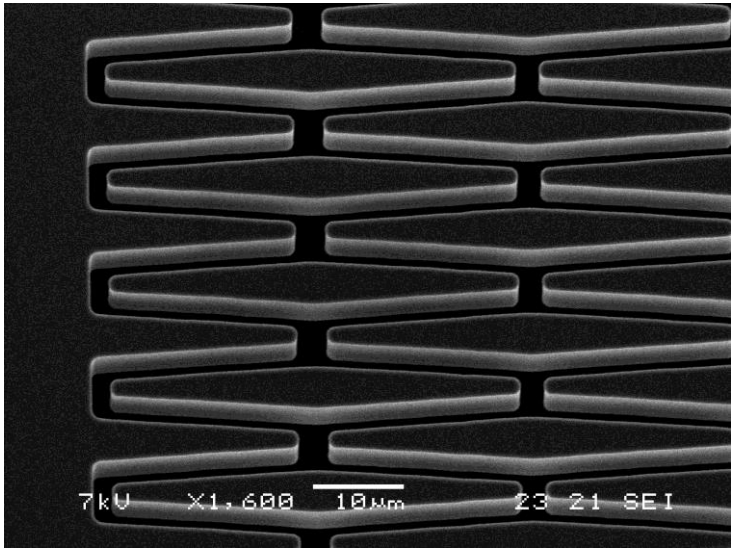

Op De Beeck, J., Callewaert, M., Ottevaere, H., Gardeniers, H., Desmet, G., De Malsche, W. (2014), J. Chromatogr. A, 1367, 118-122

Visualization of band shapes

In a pillar array filled with <u>AR 3 hexagons</u>

Injected plugs are monitored over a column length of 1 cm

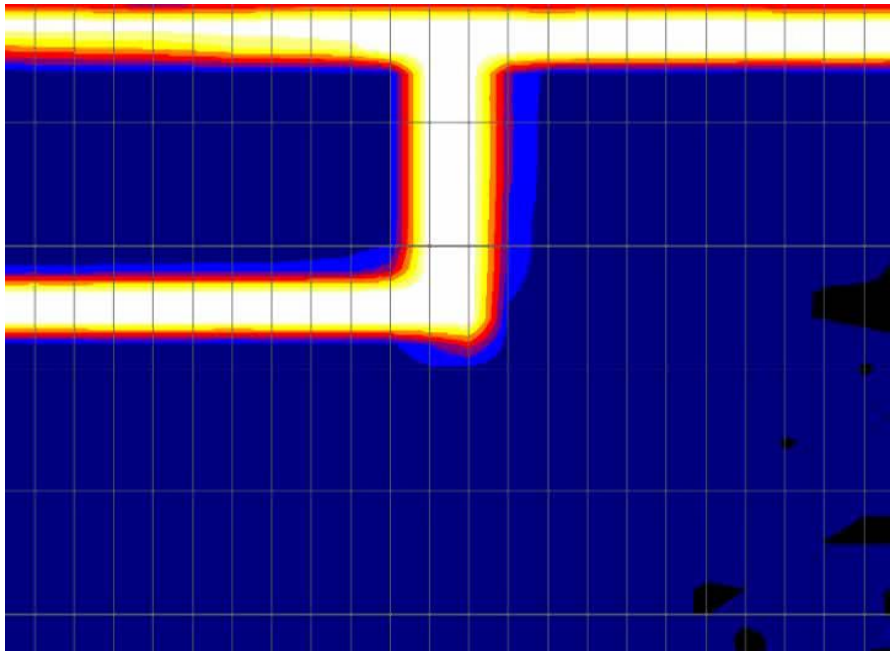

2.0 µm sidewall distance

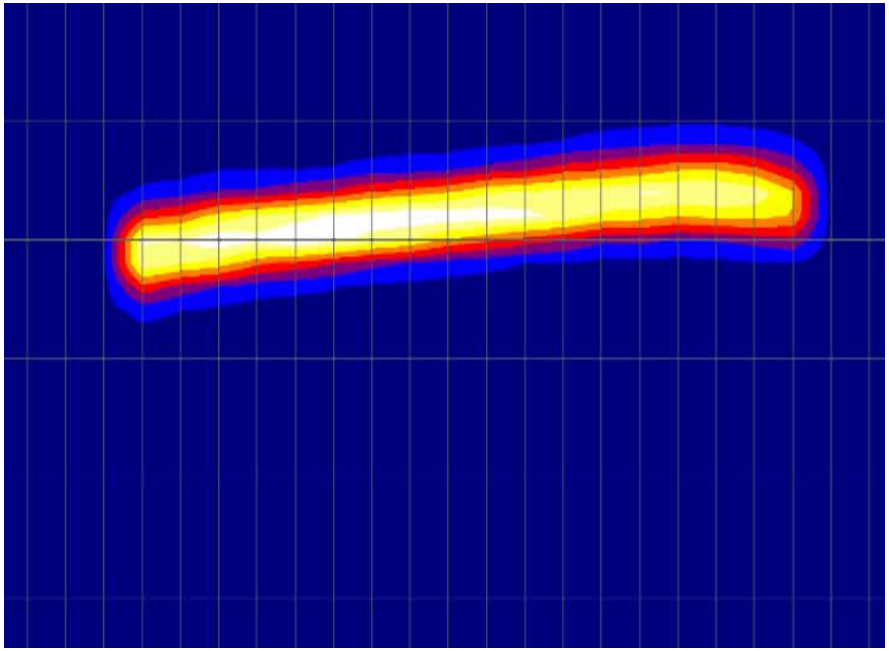

2.6 µm sidewall distance

The camera is displaced at a constant speed of 1000 µm/s

Visualization of band shapes

In a pillar array filled with <u>AR 9 hexagons</u>

Injected plugs are monitored over a column length of 1 cm

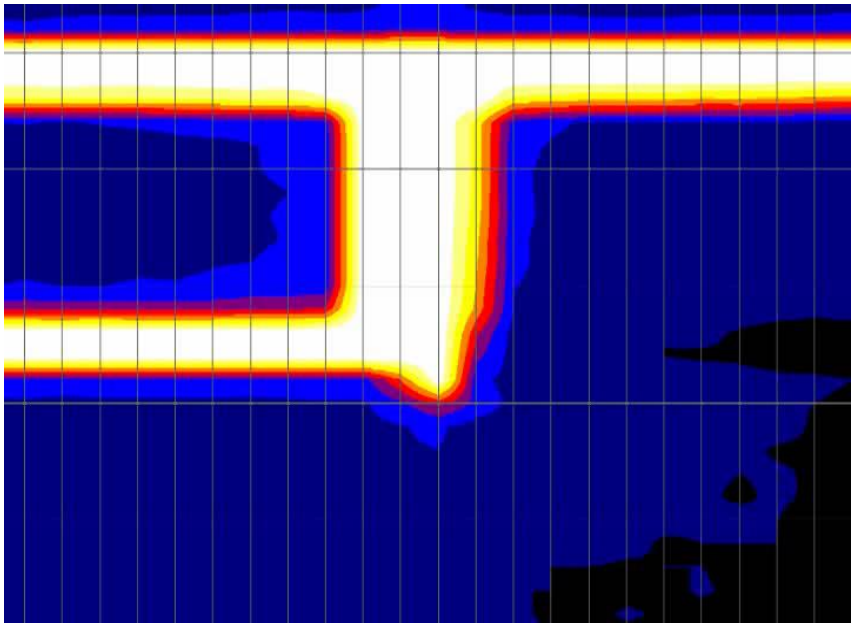

2.0 µm sidewall distance

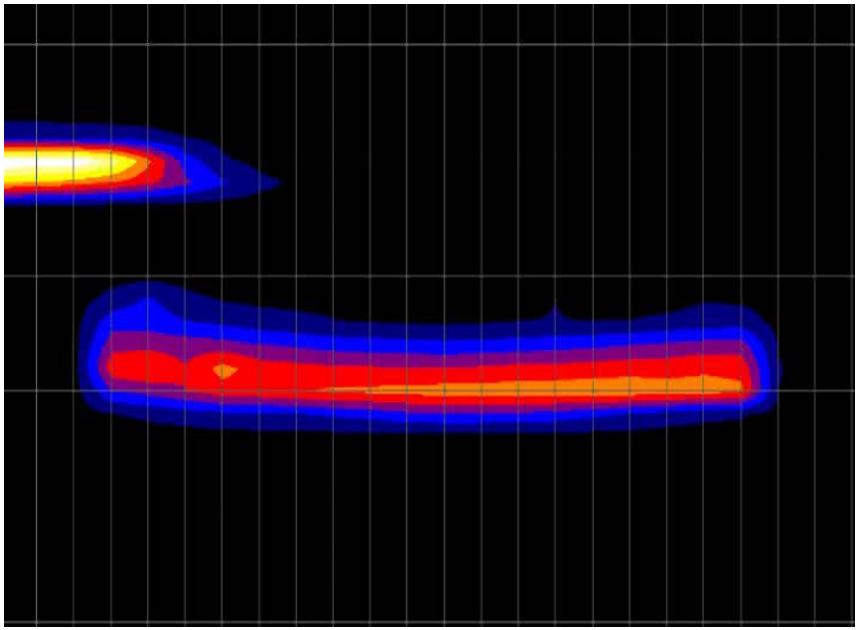

2.6 µm sidewall distance

The camera is displaced at a constant speed of 625 µm/s

Sidewall offset

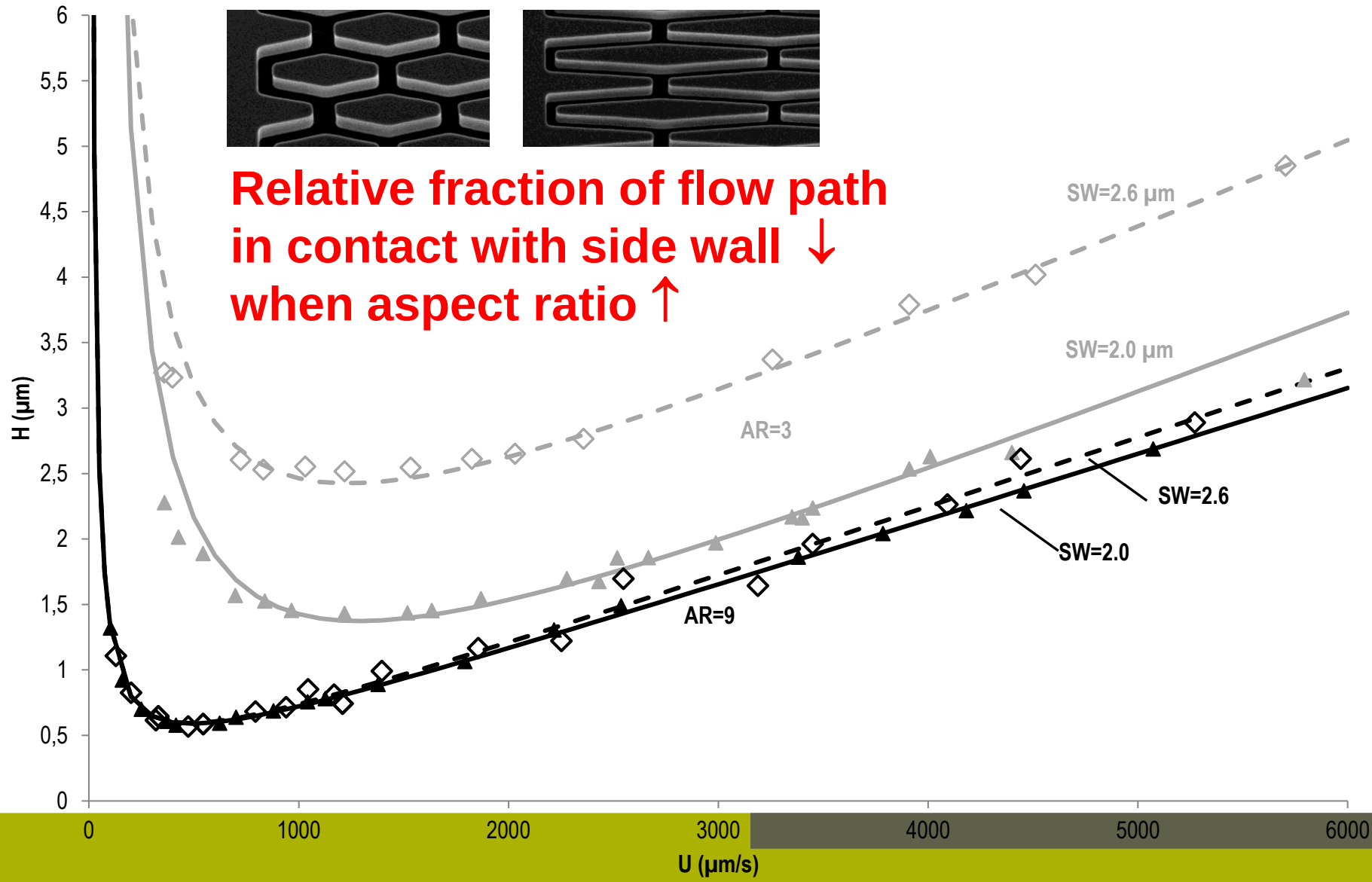

‘Unlimited’ cross sections

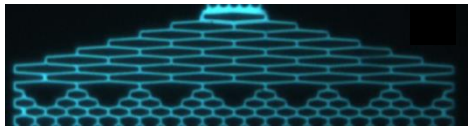

2 mm wide channel
2.3 µm spacing
depth 18 µm
AR=15
Equivalent cyl. diameter: 214 µm

0.1 mm/s

Reversed phase (C8) separation of C440, C480 (50/50 v/v MeOH/water)

Towards sub-µm H

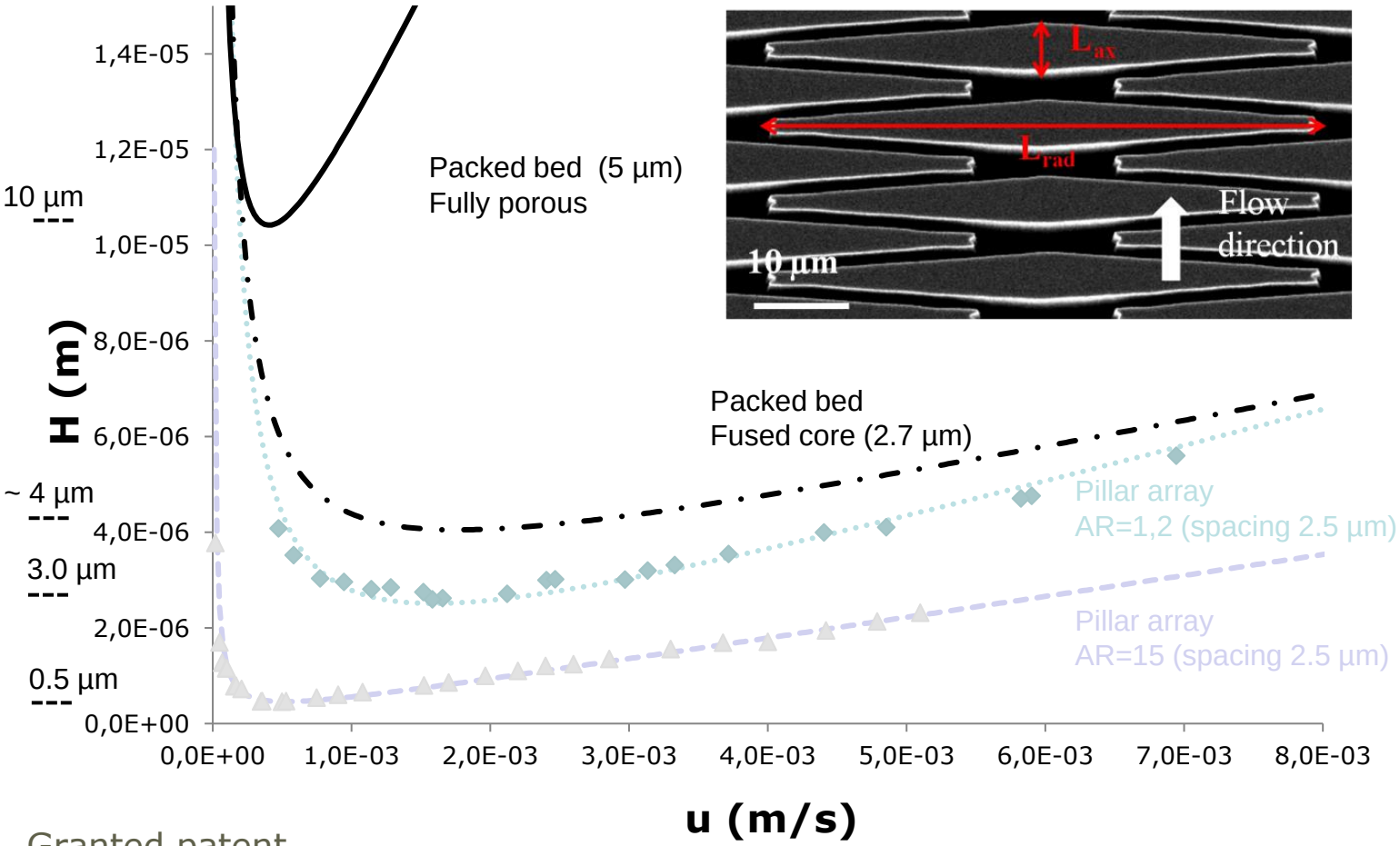

Coumarin
C480 (1mM)
MeOH

Granted patent

J. Op De Beeck, M. Callewaert, H. Ottevaere, H. Gardeniers, G. Desmet and W. De Malsche (2013), *On the Advantages of Radially Elongated Structures in Microchip-Based Liquid Chromatography*, Anal. Chem.

Vortex Liquid Chromatography

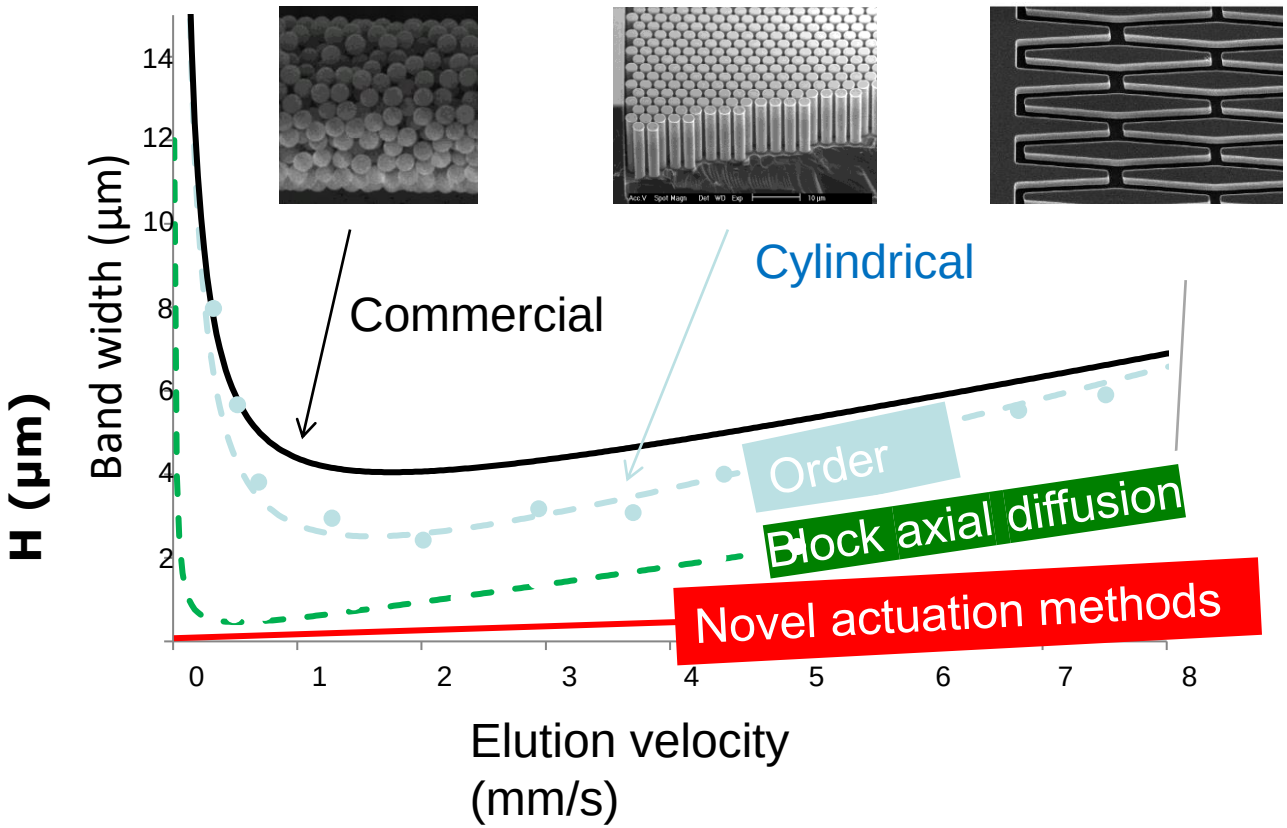

Lateral mixing to reduce dispersion

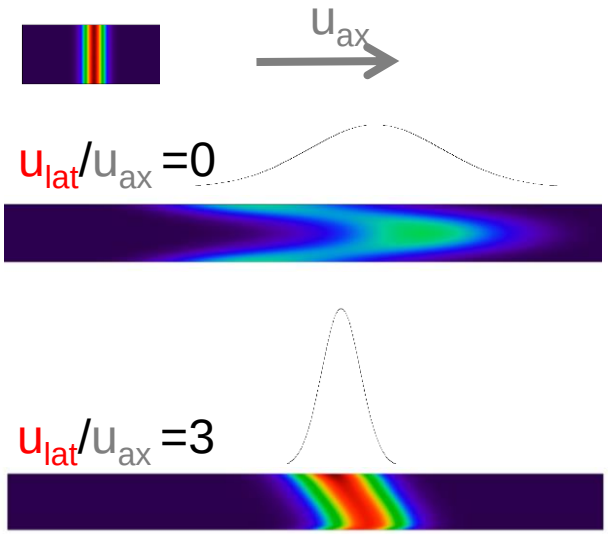

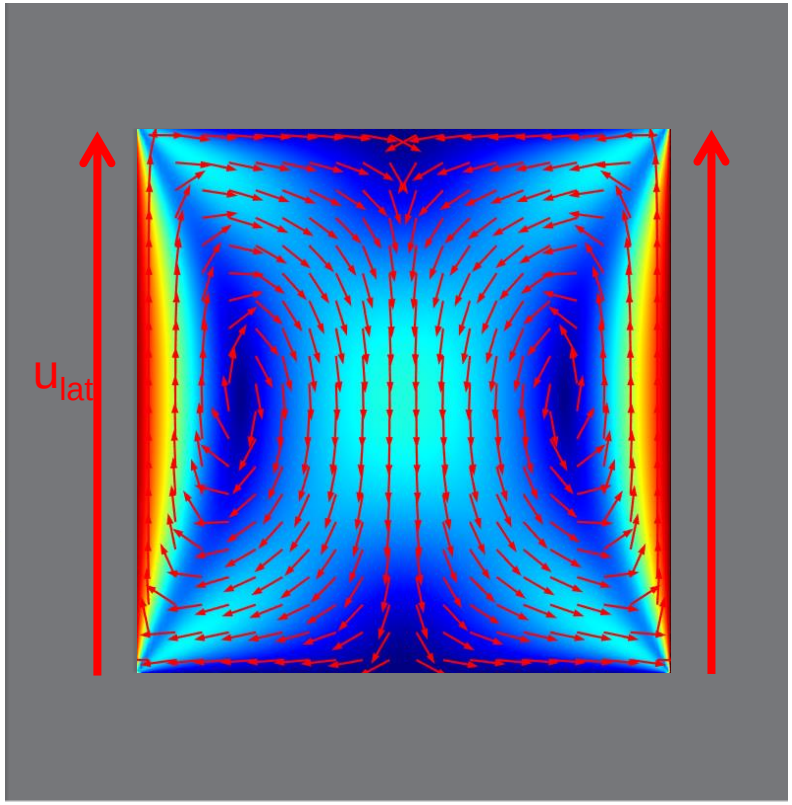

Permanent charge approach

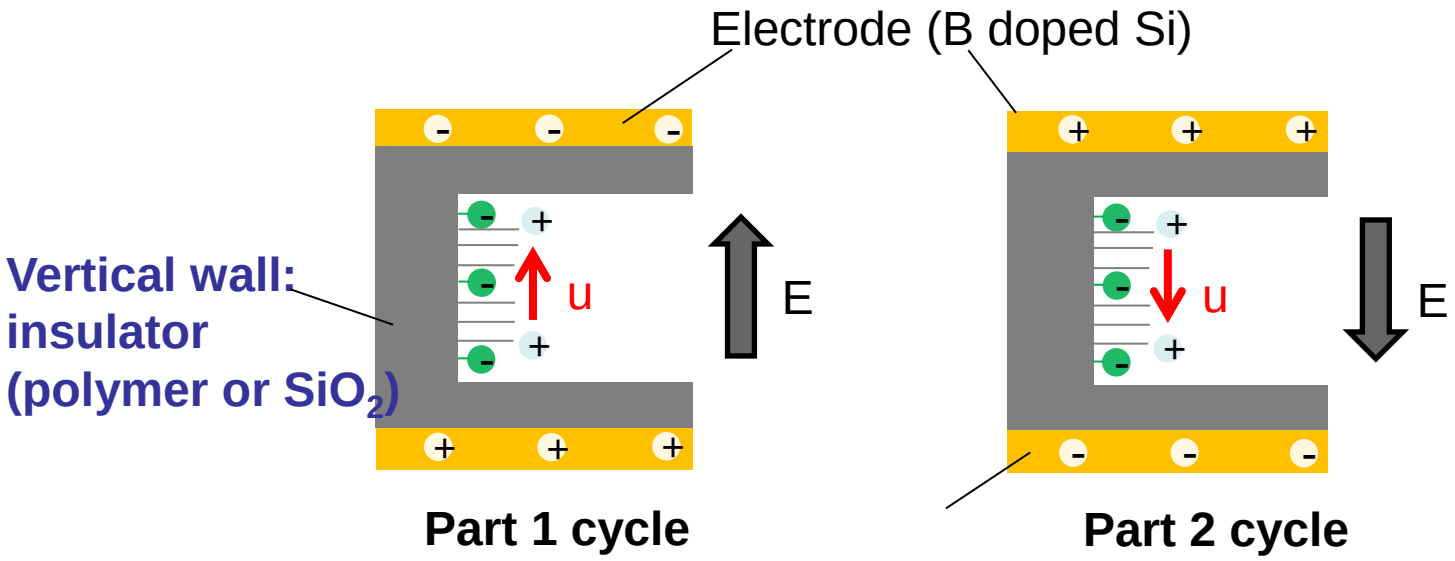

Induced charge (of support) approach

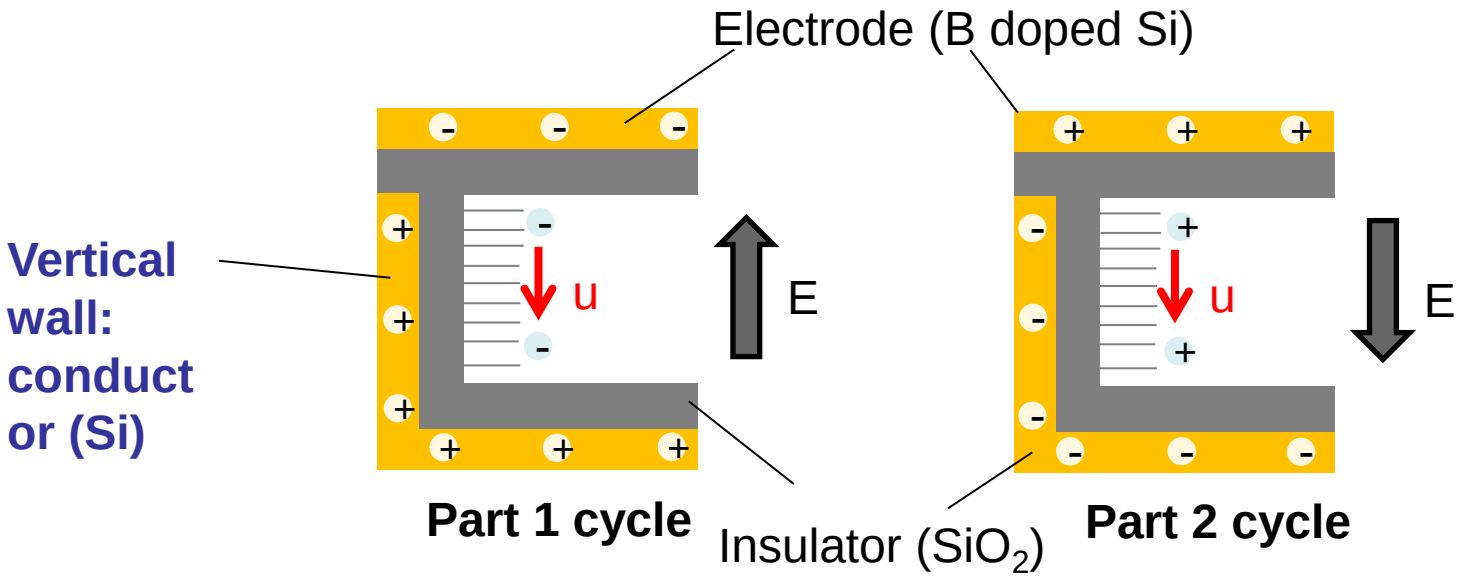

Induced charge approach

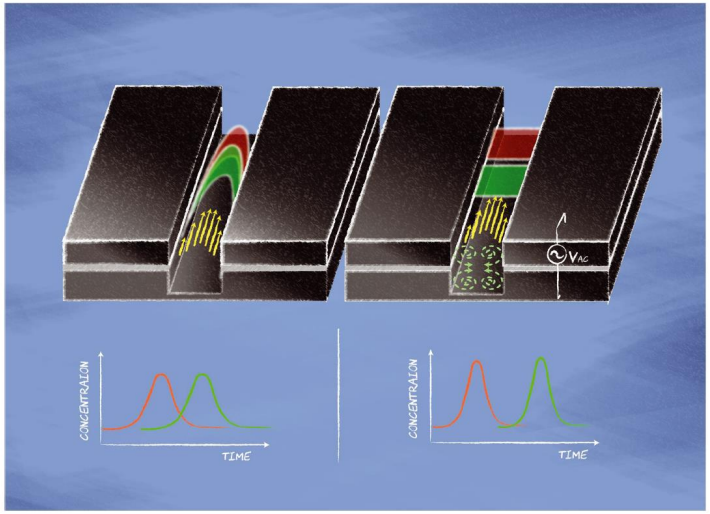

As featured in:

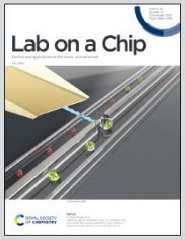

See Wim De Malsche *et al.*, *Lab Chip*, 2020, **20**, 3938.

Reduction of Taylor–Aris dispersion by lateral mixing for chromatographic applications

Dispersion of analyte sample bands that are being transported and separated in analytical devices can be largely reduced by enhancing lateral mass transport much beyond the rate of diffusion. This is achieved by inducing lateral flows with AC electroosmotic flows in a newly introduced vortex chromatography methodology.

Si vertical wall - µfabrication

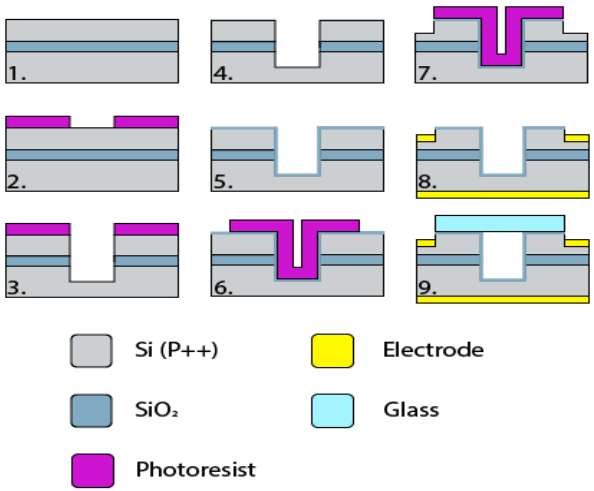

Fig 2. Manufacturing process of the chip 1. P++ SOI wafer as a substrate. 2. Standard lithography 3. Dry etching of the channel. 4. Stripping of photoresist 5. Thermal oxidation of silicon. 6. Spray-coating of photoresist and lithography. 7. Dry etching electrode pads. 8. Sputtering of Ti/Pt layer and lift-off. 9. Anodic bonding of Borosilicate glass to the patterned Si substrate

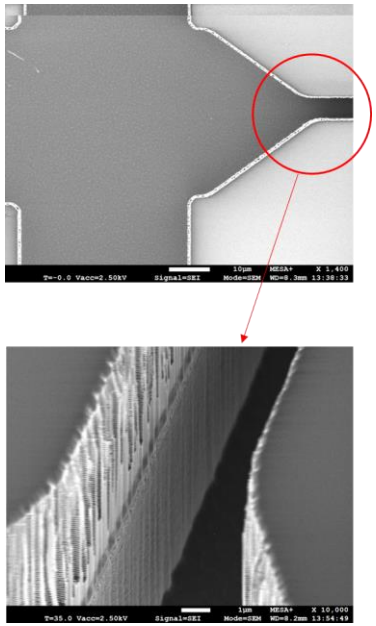

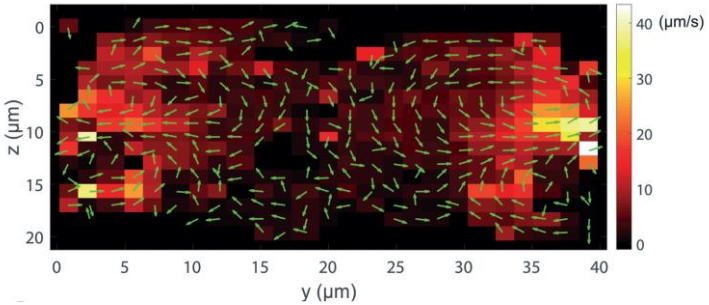

Westerbeek, E., Bomer, J.G., Olthuis, W., Eijkel, J.E., De Malsche, W. (2020), Reduction of Taylor-Aris dispersion by lateral mixing for chromatography applications, Lab-on-a-chip, 20, 3938 – 3947

Flow visualization

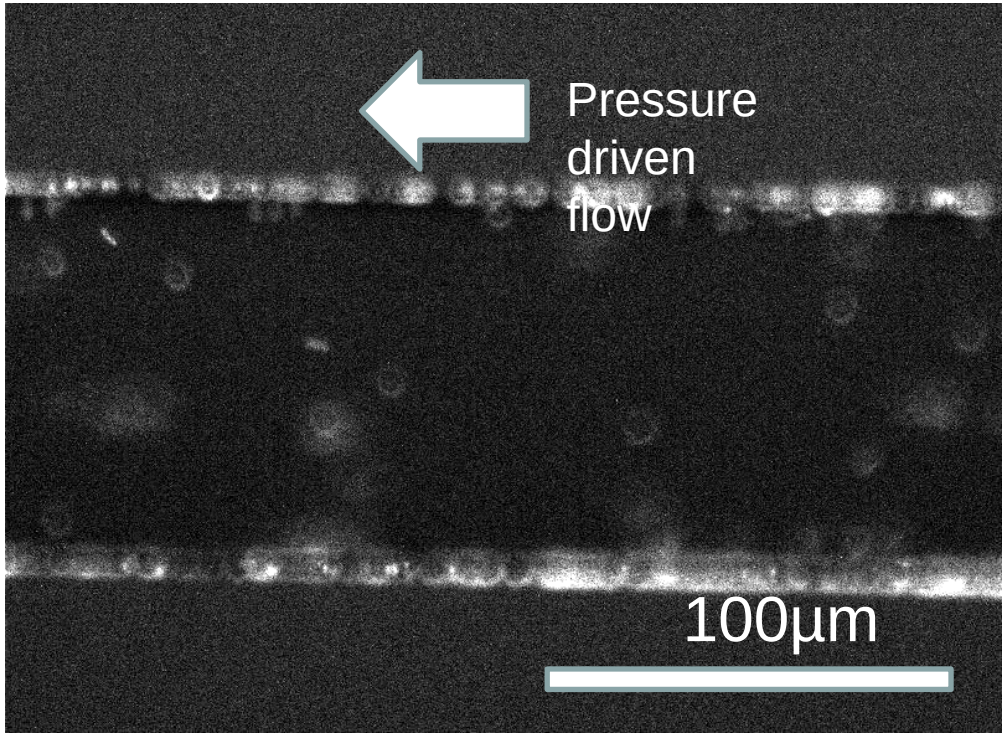

Dispersion reduction with lateral flows

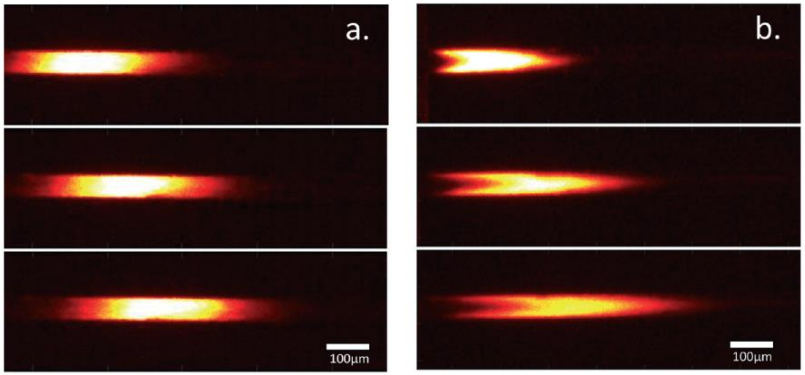

AC-EOF *No AC-EOF*

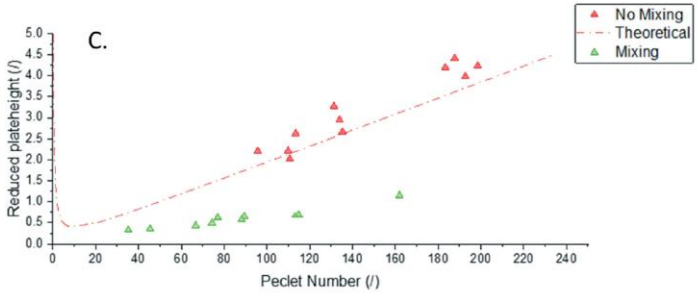

Fig. 5 Dispersion of FITC-dextran a) fluorescent intensity of an injected plug of FITC-dextran (20 kDa) subject to pressure driven flow with an induced lateral AC-EOF the AC-potential was applied right after the injection was performed. b) Fluorescent intensity of an injected plug of FITC-dextran (20 kDa) subject to pressure driven flow without an induced lateral flow. c) Reduced plate height values at different axial Peclet numbers, with and without lateral mixing. The theoretical plate height is displayed for a channel with aspect ratio 2. Experiments were performed with FITC-dextran 20 kDa, the applied voltage was 10 V-pp at 10 kHz.

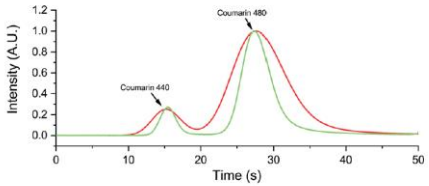

Fig. 6 Chromatographic separation of coumarin 440 & 480 fluorescence intensity over time without AC-electroosmotic flow (red) and with electroosmotic flow (green). The mixture injected contained coumarin 440 and coumarin 480. The point of analysis was 2 mm downstream from the point of injection.

Permanent charge (of support) approach

Vertical wall:
Suppressed flow

Sloped wall:
sustained flows

Sloped wall:
sustained flows

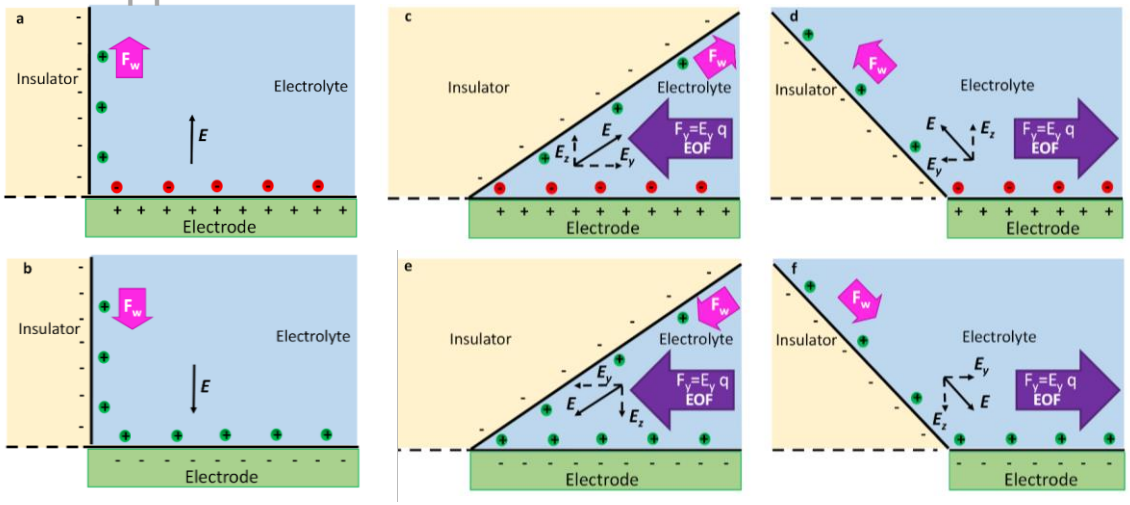

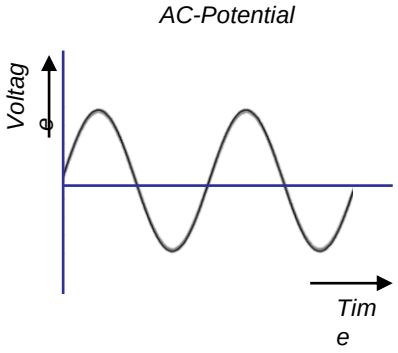

$$u_{eof} = \frac{\sigma_t E_t}{\eta \kappa}$$

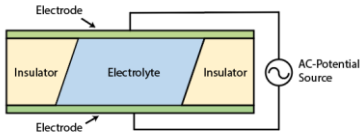

Polymer approach - flow profile

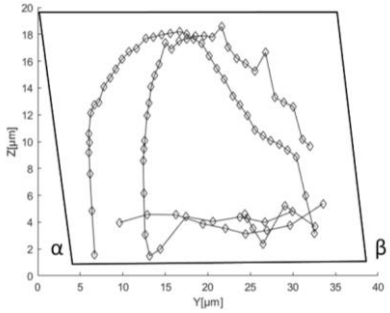

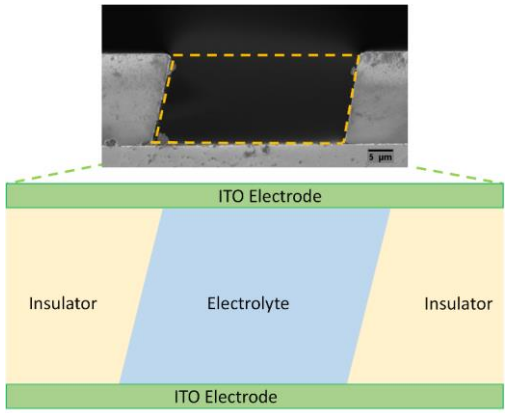

Figure 4: Cross sectional SEM images of the parallelogram shaped device. The image displays the device device before bonding the top electrode.

Shaping vortex organization

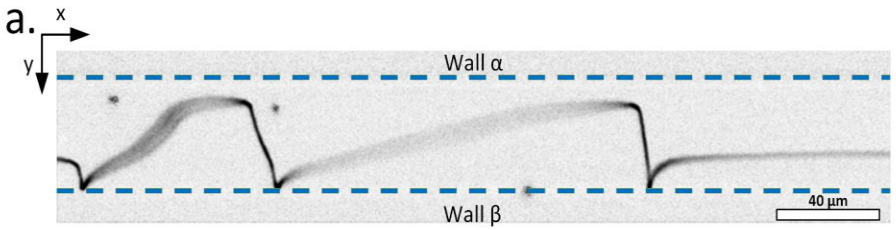

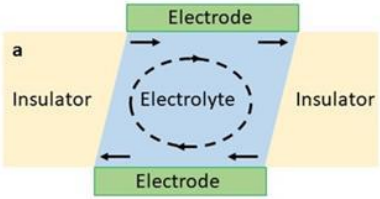

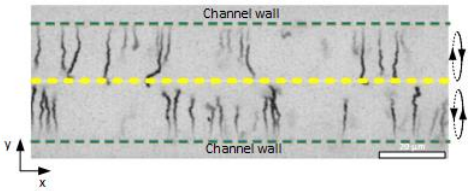

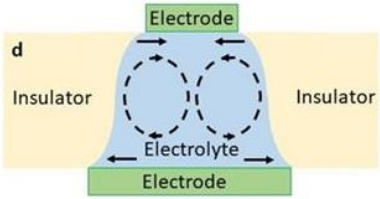

Control of vortices by channel cross section

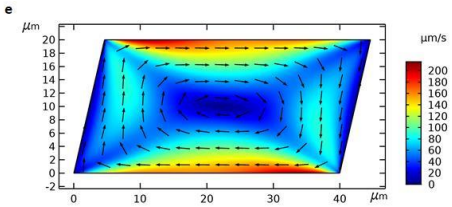

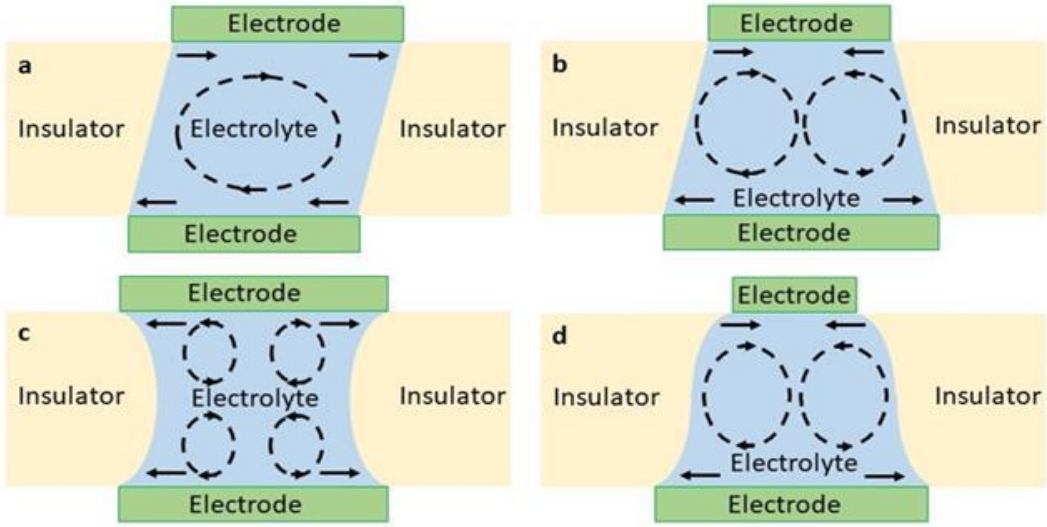

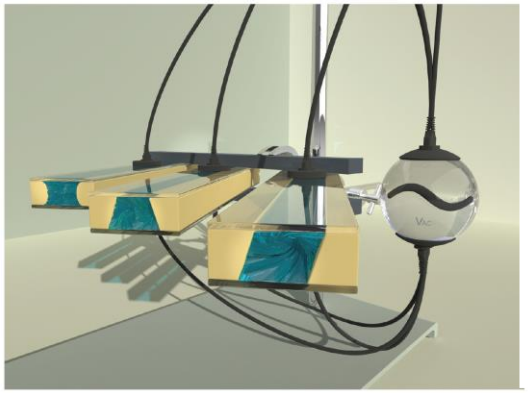

As featured in:

See Wim De Malsche *et al.*, *Lab Chip*, 2021, **21**, 3105.

Inducing AC-electroosmotic flow using electric field manipulation with insulators

A 3D-shaped insulating spacer is incorporated in a microchannel with two parallel transparent electrode walls, allowing to induce AC-electroosmotic flow. Interestingly, the presence of non-vertical walls is a critical requirement to induce vortex flows, and the shape of the channel determines the resulting vortex organization, including the number of vortices.

Tiflidis, C., Westerbeek, E., Jorissen, K., Olthuis, W., Eijkel, ,J., De Malsche, W. (2021),
Inducing AC-electroosmotic flow using electric field manipulation with insulators, Lab-on-a-chip, 2021,21, 3105-3111

PARTICLE SEPARATION AND HANDLING

H-Filter

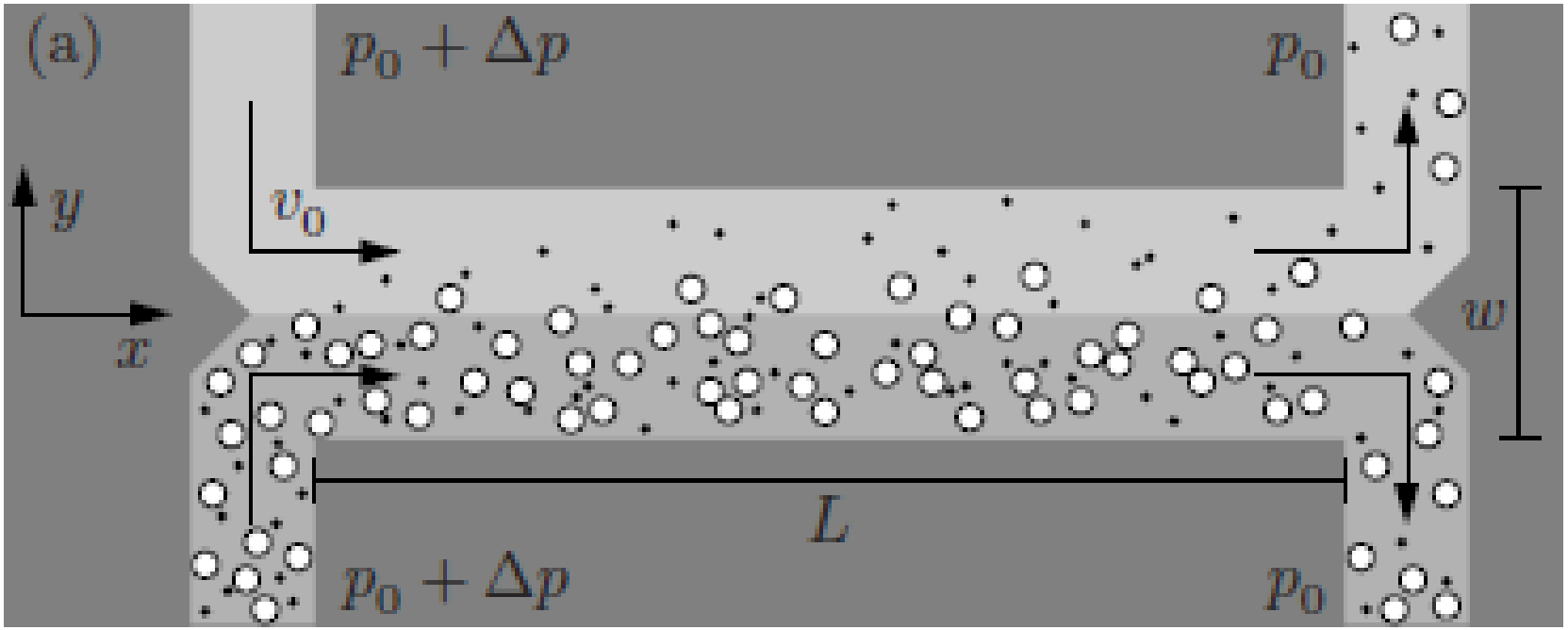

Flow Field flow fractionation (AF4)

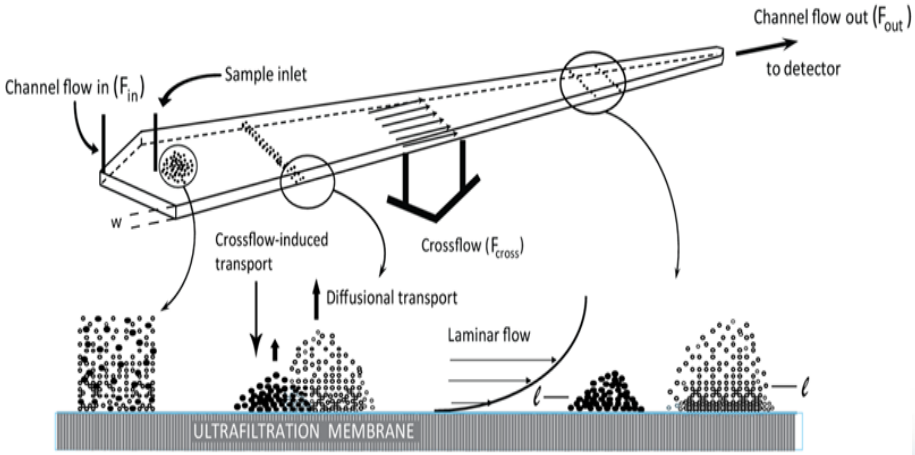

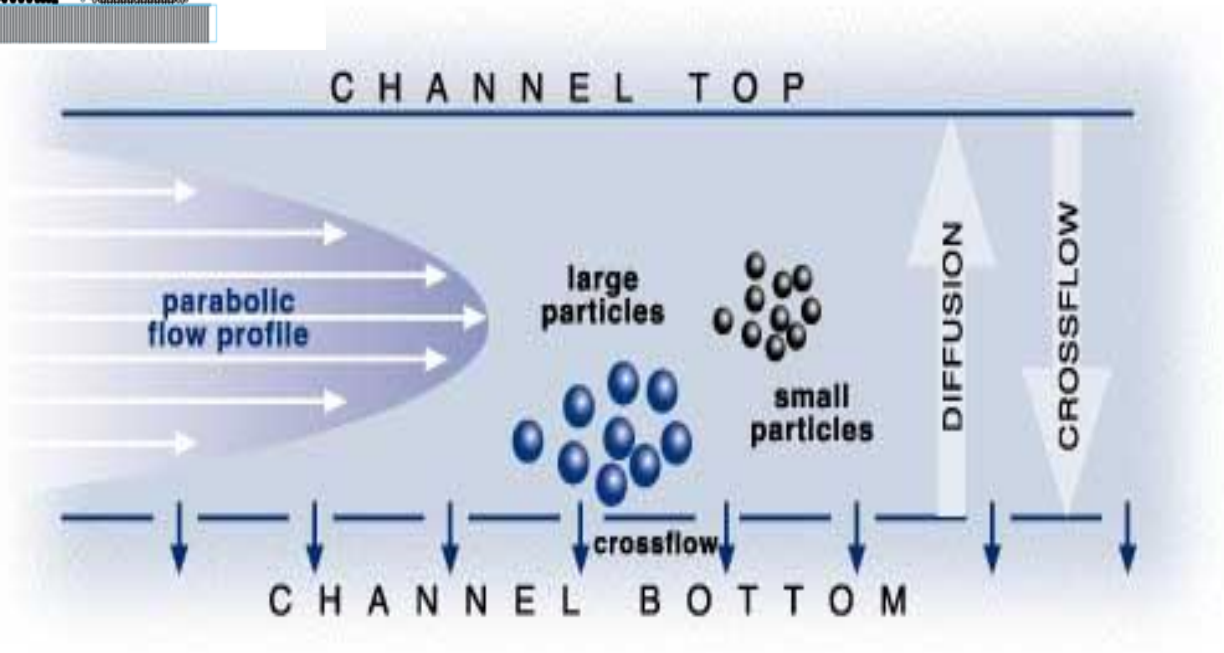

Pinched flow fractionation

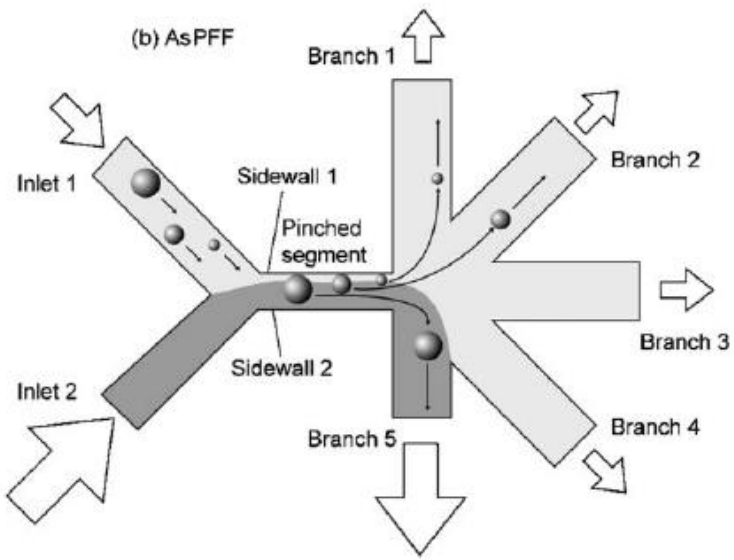

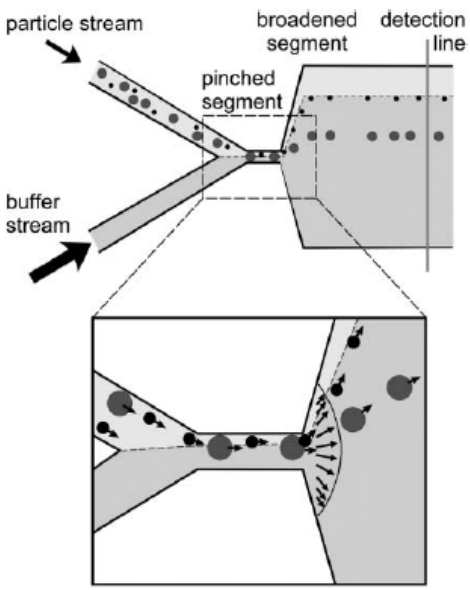

Fig. 2 The principle of pinched flow fractionation for the separation of microparticles or cells, based on laminar flow behaviour and negligible diffusion of the particles. A buffer stream and a particle carrying stream are forced through a narrow, pinched channel segment before entering a widening channel. Due to the higher flow rate of the buffer stream, the particles are pushed against the wall of the pinched segment and are thus transported into specific laminar flow streams based on their size. This difference is enhanced as the particles enter the widening channel. Redrawn with permission from ref. 10, copyright 2004, American Chemical Society.

Seki et al, Lab Chip, 2005, 5, 778–784

Ratchets: principle

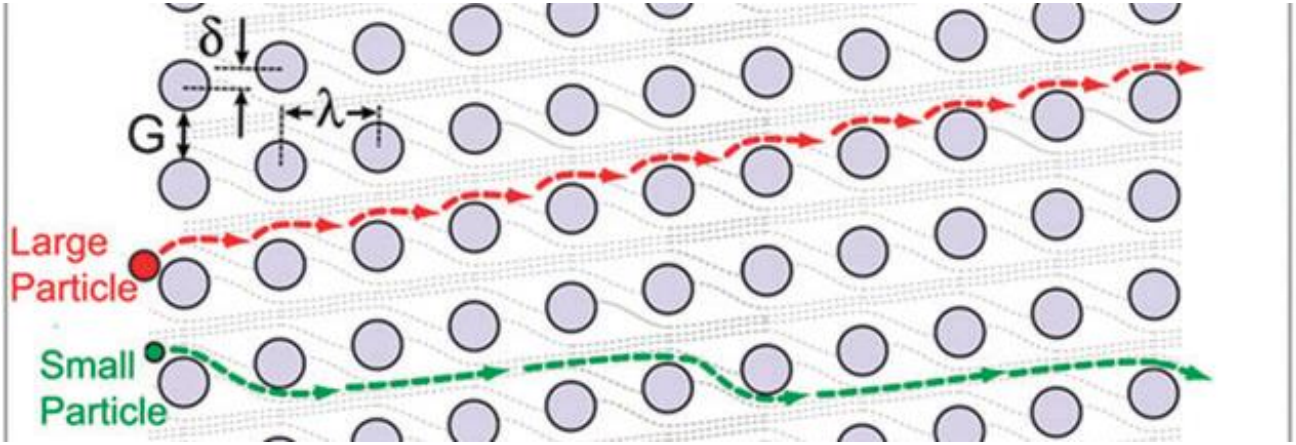

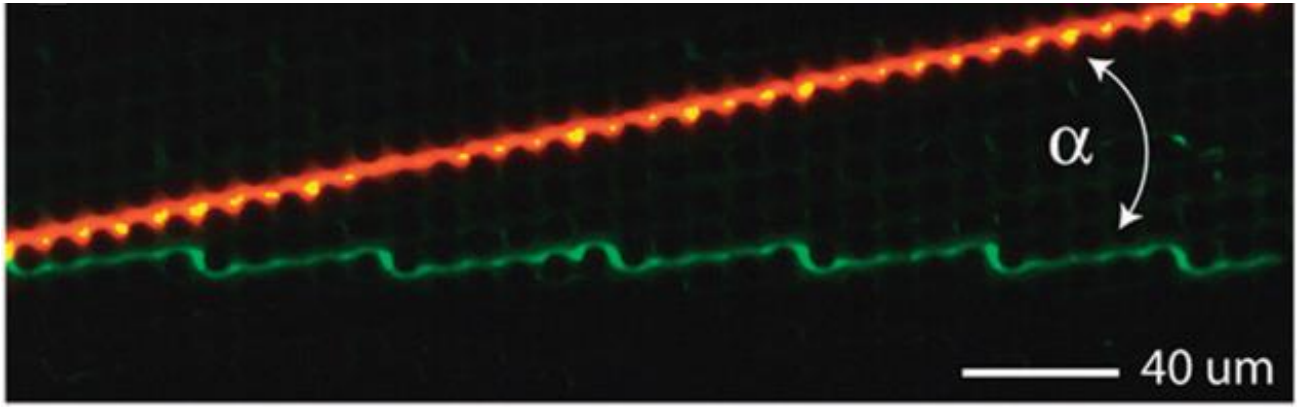

www.sciencemag.org SCIENCE VOL 304 14 MAY 2004

Ratchets

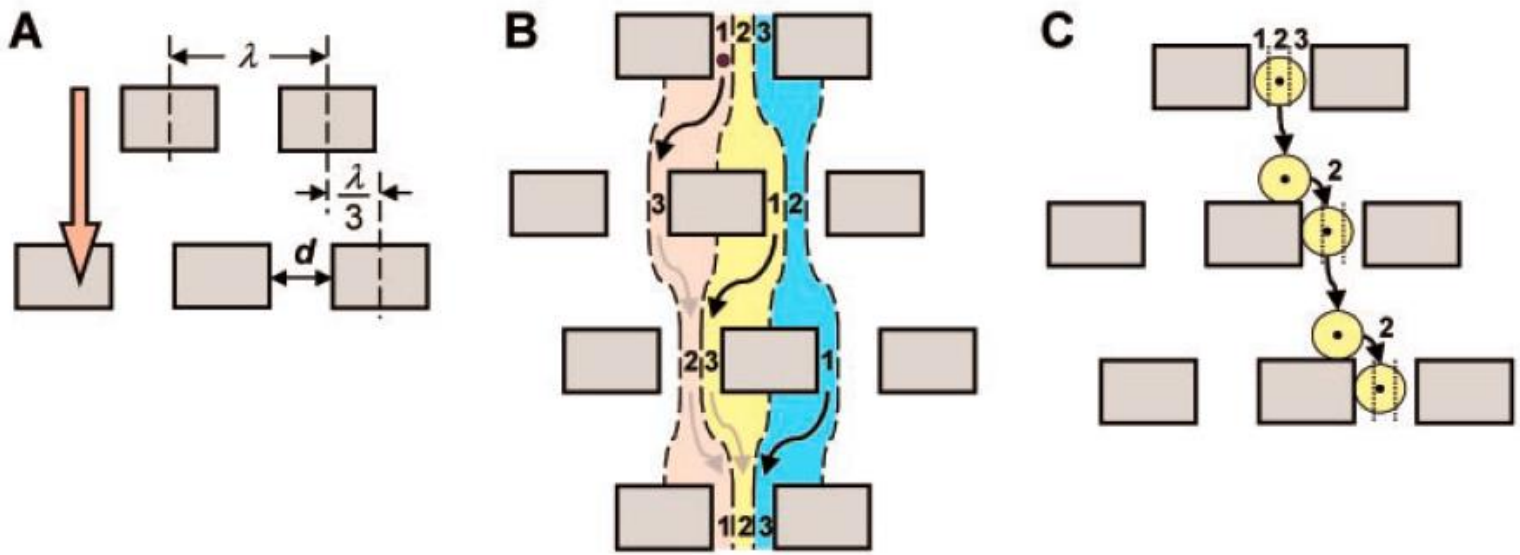

Fig. 1. (**A**) Geometric parameters defining the obstacle matrix. A fluid flow is applied in the vertical direction (orange arrow). (**B**) Three fluid streams (red, yellow, and blue) in a gap do not mix as they flow through the matrix. Lane 1 at the first obstacle row becomes lane 3 at the second row, lane 3 becomes lane 2 at the third row, and so on. Small particles following streamlines will thus stay in the same lane. (**C**) A particle with a radius that is larger than lane 1 follows a streamline passing through the particle's center (black dot), moving toward lane 1. The particle is physically displaced as it enters the next gap. Black dotted lines mark the lanes.

Ratchets: principle

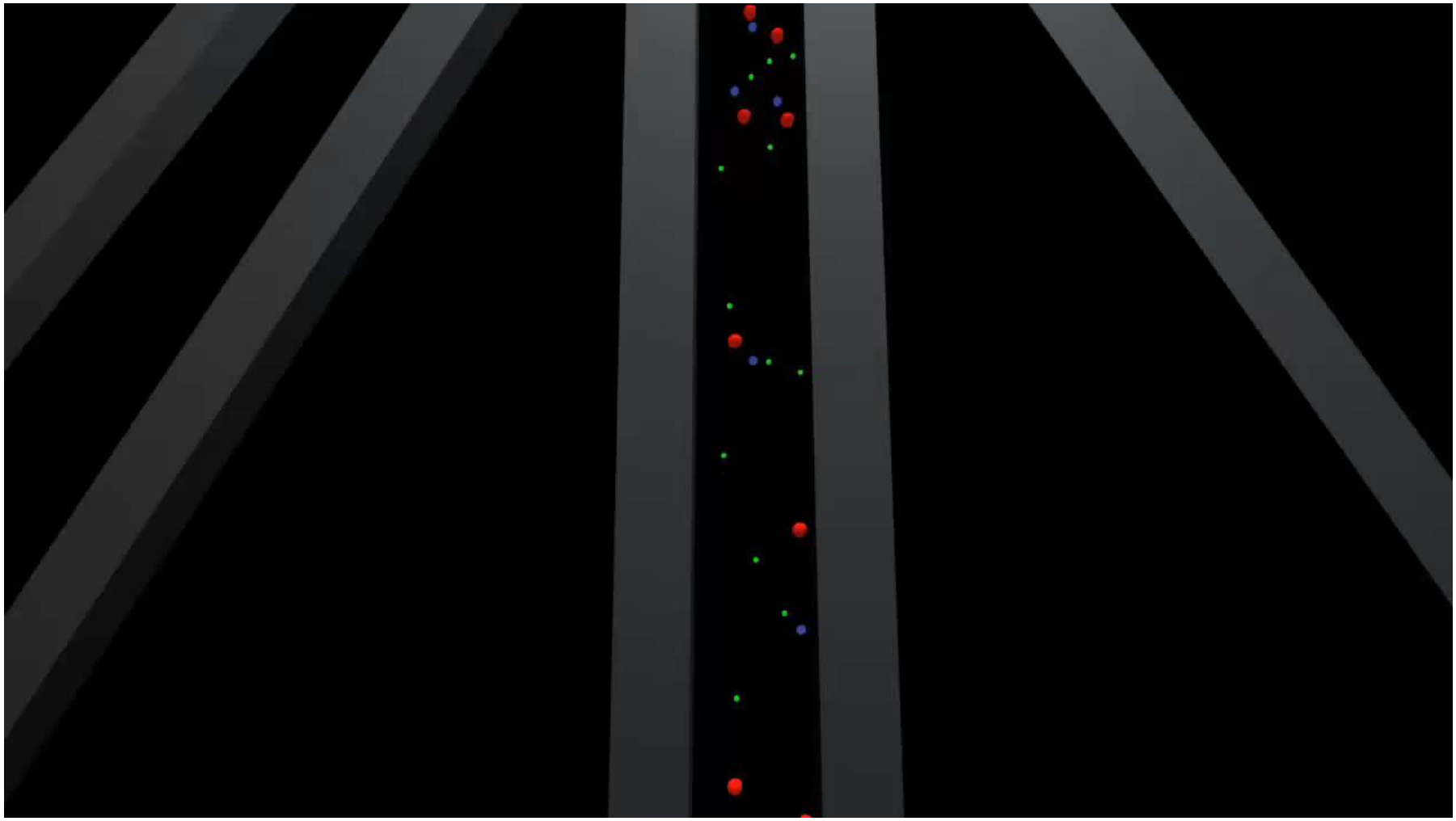

Continuous nanoparticle separations

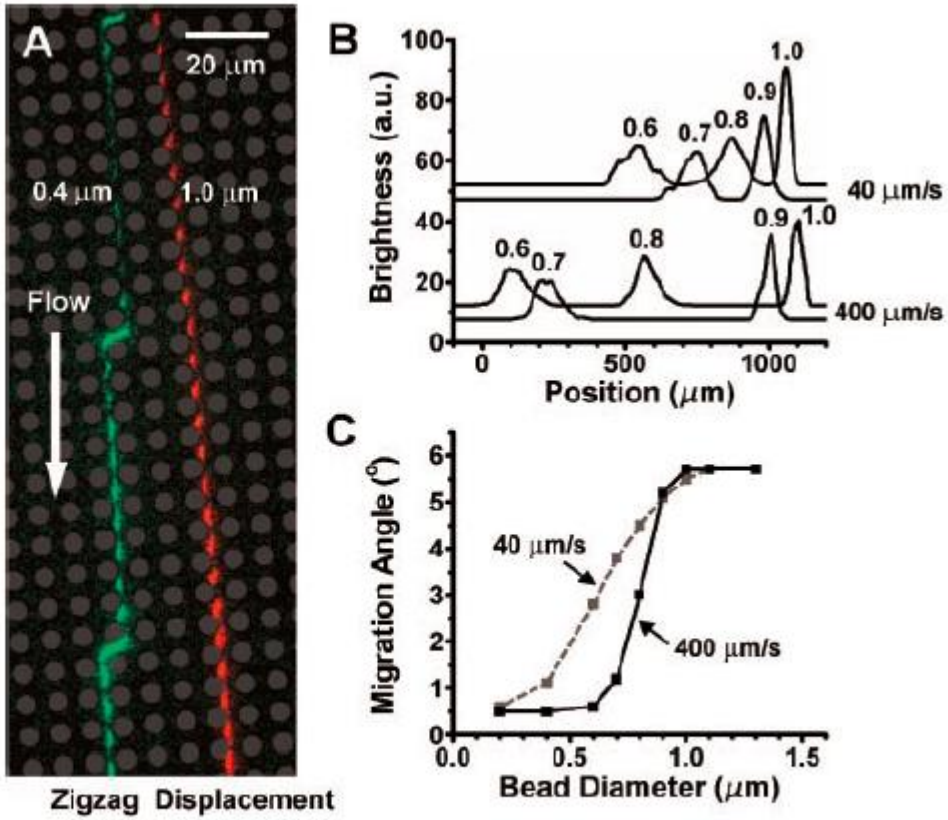

Fig. 2. (A) Fluorescent images of microspheres migrating in the matrix, showing trajectories of the two transport modes. The flow speed is ~400 μm/s, created by a pressure of 30 kPa. The gray dots, which represent the obstacles, are superimposed on the fluorescent image. (B) Fluorescence profiles of microspheres separated with flow speeds of ~40 μm/s (upper curves) and ~400 μm/s (lower curves) scanned at ~11 mm from the injection point. The beads with diameters of 0.60, 0.80, and 1.03 μm are green fluorescent, whereas those with diameters of 0.70 and 0.90 μm are red, and thus each scan is shown as two curves representing the two colors. a.u., arbitrary units. (C) Measured migration angles as a function of microsphere diameter at two different flow speeds.

Ratchets: concentration

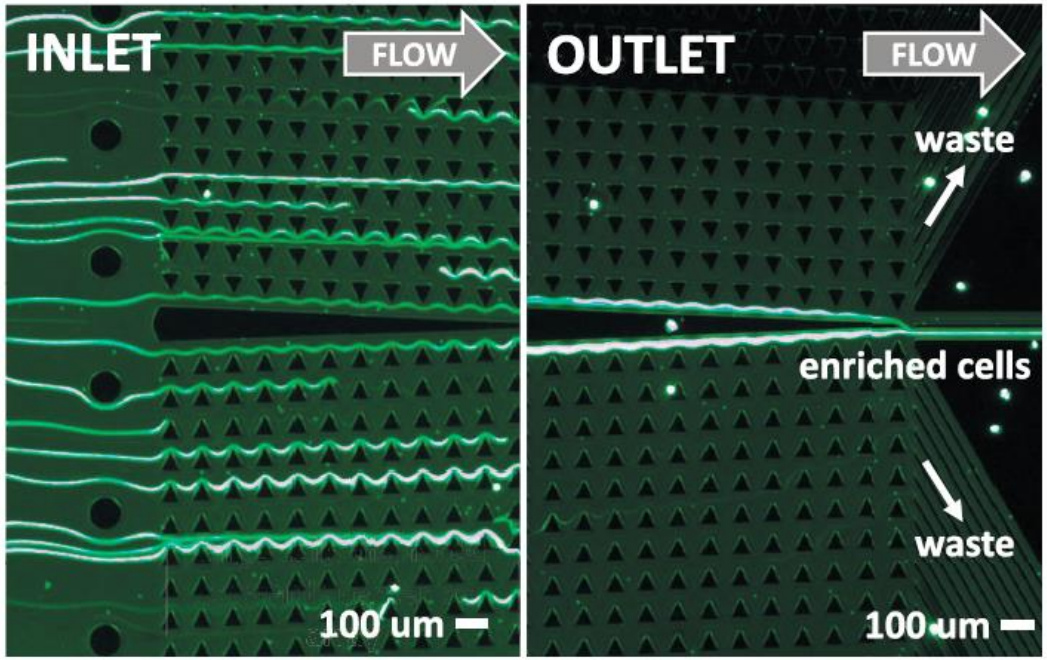

FIG. 3. **CTC enrichment in DLD array**. Trajectories of GFP-expressing MDAMB231 breast cells in an array with 42 μm gaps, 1/20 array tilt, and 7 μm critical particle size at device inlet and outlet at flow rate of 500 $\mu L/min$. Cells are evenly dispersed at inlet but are concentrated against central wall at outlet and directed to narrow collection outlet.

AIP ADVANCES **2**, 042107 (2012)

Deterministic separation of cancer cells from blood at 10 mL/min

Kevin Loutherback,[1,2,a] Joseph D'Silva,[1,2] Liyu Liu,[1,3] Amy Wu,[1,2] Robert H. Austin,[1,3,b] and James C. Sturm[1,2]

6 x increase in concentration

19 µm cells

0,5 ml/min
Tested up to 10 ml/min

Coulter counter. From an initial concentration of 3.75×10^6cells/mL with average size 19.5 μm, the collection output had a concentration of 2.1×10^7 cells/mL with average size 19.5 μm while waste output had a concentration of 3.7×10^5 cells/mL with average size 19.0 μm. Factoring in the volume of each output ($V_c = 0.8$ mL, $V_w = 4.2$ mL), we can calculate the capture efficiency as the ratio of cells in the collection output to the total number of cells in both outputs $\frac{\#\,collected\ cells}{total\ cells} = \frac{C_c V_c}{C_c V_c + C_w V_w}$. Using this definition, 91% of the targeted cells were collected by the device.

Inertial microfluidics

- High Reynolds numbers (1<Re<100) in microfluidics
- Inertia creates a lift force which locates the particles at certain equilibrium positions.
- 4 equilibrium positions in square microchannels

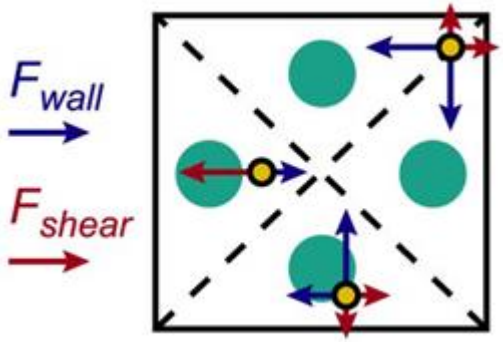

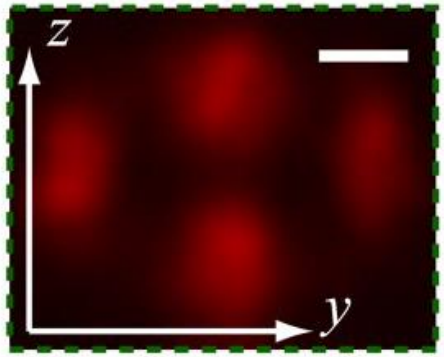

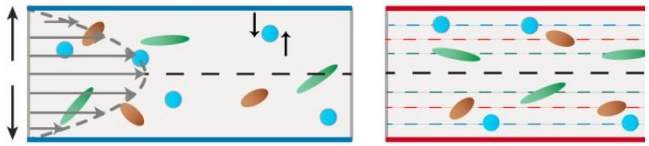

PNAS, 104(48), **2007**, 18892-18897

Inertial microfluidics: spiral

- Fractions will be enriched
- Solutions with particles with multiple sizes can be separated

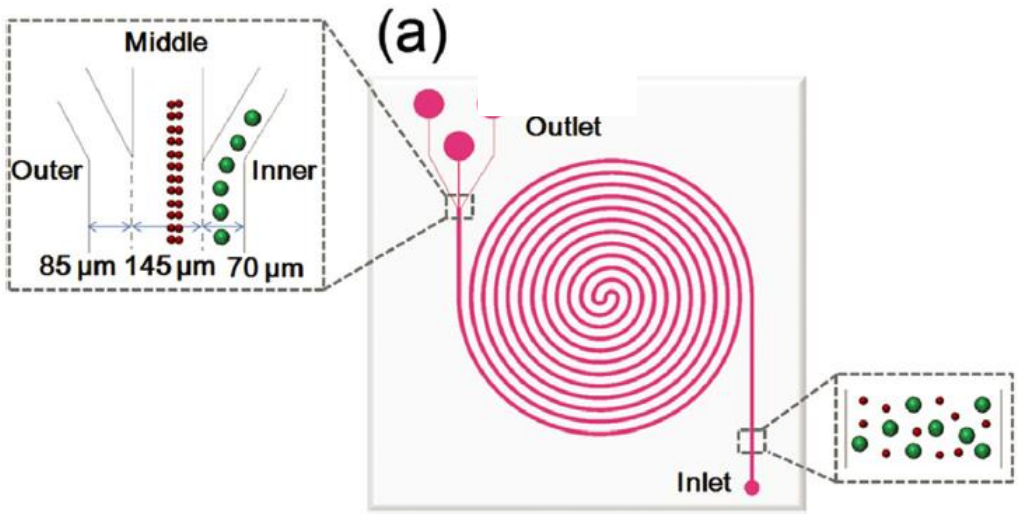

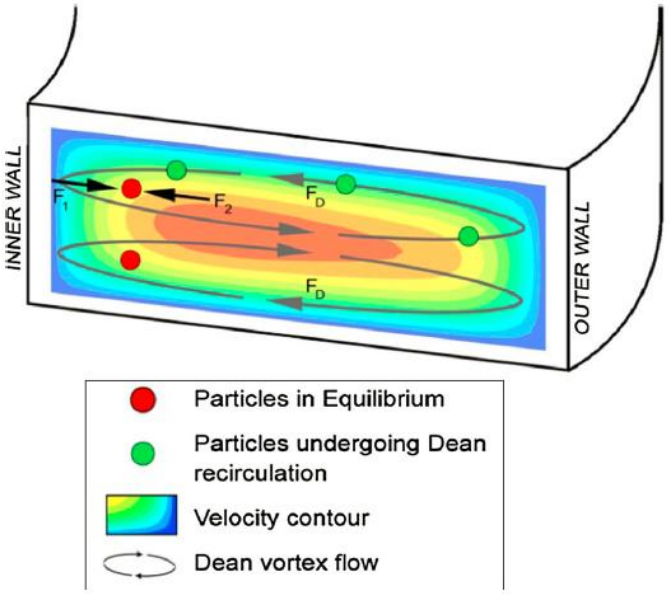

Serpentine

- Equilibrium positions also determined by secondary rotational flow in turns
- Dean number

$$De = Re\left(\frac{D_H}{2r}\right)^{1/2} > 1$$

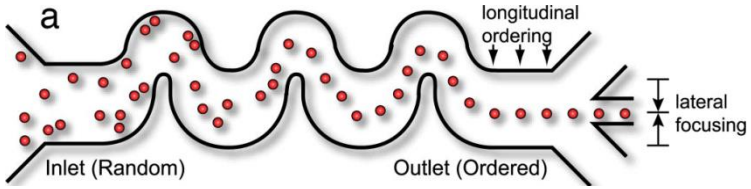

PNAS, 104(48), **2007**, 18892-18897

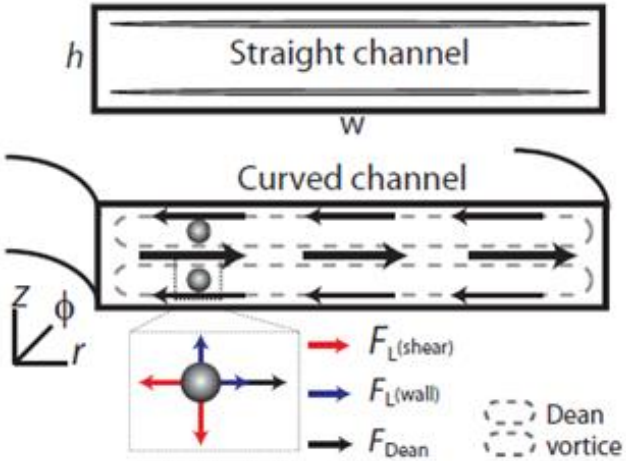

- Focusing depends on channel and particle Reynolds number
- Re_p<1 does not focus

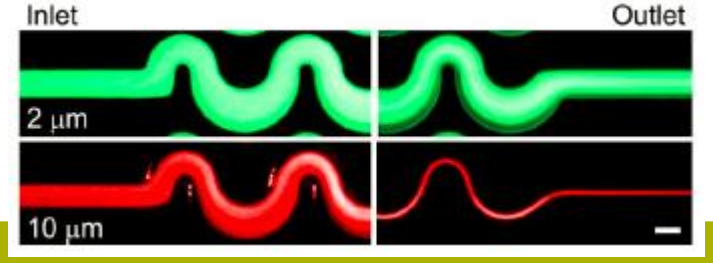

PNAS, 104(48), **2007**, 18892-18897

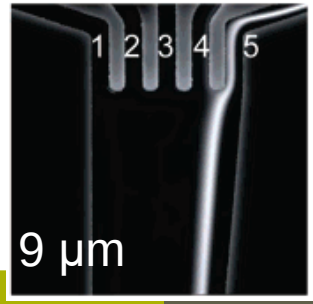

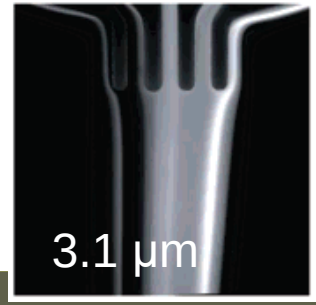

Anal. Chem., 80(6) **2008**, 2204-2211

Conclusions

- Different flow propulsion methodes, selection by:
  - Desired separation method
  - Detection
  - Solvent compatibility
  - Pressure, voltage, … limitation
- Imperfections can have huge impact on performance
- Many opportunities in terms of detection and separation
- Vortices key to overcome diffusion limitations